Available online at www.sciencedirect.com
ScienceDirect
Radiation Physics and Chemistry 77 (2008) 225–244
Radiation Physics and Chemistry
www.elsevier.com/locate/radphyschem

Review

Irradiation treatment of azo dye containing wastewater: An overview

László Wojnárovits, Erzsébet Takács*

Institute of Isotopes, Hungarian Academy of Sciences, H-1525 Budapest, P.O. Box 77, Hungary

Received 2 March 2007; accepted 7 May 2007

Abstract

The radiation-induced decolouration and degradation of aqueous solutions of azo dyes and their model compounds (anilines, phenols, triazines) are reviewed together with practical applications and the experimental methods (pulse radiolysis, steady-state gamma radiolysis, as well as end-product analysis) used for studying the reactions. The proposed mechanisms and the rate coefficients for the reactions of $^{\bullet}OH$, e^{-}_{aq} and $^{\bullet}H$ water radiolysis intermediates with the dye molecules and with model compounds are summarized.

Keywords: Azo dyes; Irradiation treatment; Decolouration; Degradation; Mineralization; Advanced oxidation processes (AOP)

1. Introduction

Azo dyes are frequently used for dyeing fabric therefore they are expected to be adherent, long lasting, and resistant to sunshine and chemical processes, in the case of dyed fabric it is required that the dyes should not fade through oxidation in the normal washing process. However, it is of special importance that these dyes could be removed from industrial effluents. For this purpose, either sorption (Aksu, 2005; Solpan and Kölge, 2006) or degradation, e.g., by treating with one-electron oxidants have been employed. In the so-called advanced oxidation processes (AOP) for the degradation of organic pollutants, highly reactive species, mainly hydroxyl radicals are used as primary oxidants. Radiation treatment belongs to the class of AOP.

Radiation processing is extensively used in industry to produce a wide range of products. Use of radiolysis in the environmental remediation of wastewater, contaminated soil and sediment is a promising treatment technology; the chemistry behind these technologies is under extensive investigation. Together with the removal of target chemical contaminant, one should also concern the elimination of a series of intermediates of progressively higher oxygen-to-carbon ratios that are involved in the conversion of an organic molecule to CO_2. Therefore, it is essential to improve substantially our basic understanding of the radiation chemistry of dyes (reactions, pathways, and rates) in various systems.

The purpose of this work is to make a review on the results obtained both at our laboratory and at other laboratories on the degradation of azo dyes with special emphasizes on radiation degradation of H-acid containing azo dyes. For better understanding of the mechanism of degradation of the large dye molecules our knowledge on the reactions of smaller constituents of the dye molecules are also summarized. Although we mainly refer to radiolysis results, the undergoing processes, the reaction mechanisms are also relevant to other AOP. Some of the AOP are summarized in Fig. 1 and Table 1. The issues involved here are: (1) establishing the mechanisms of free radical reactions such as those applicable to remediation processes and (2) improving the overall efficiency of remediation by controlling the reactivity and the generation of free radicals.

1.1. Advanced oxidation processes

Radiation treatment of polluted waters belongs to the class of AOP. Other frequently used methods employed to

*Corresponding author. Tel./fax: +361 392 2548.
E-mail address: takacs@iki.kfki.hu (E. Takács).

0969-806X/$ - see front matter © 2007 Elsevier Ltd. All rights reserved.
doi:10.1016/j.radphyschem.2007.05.003

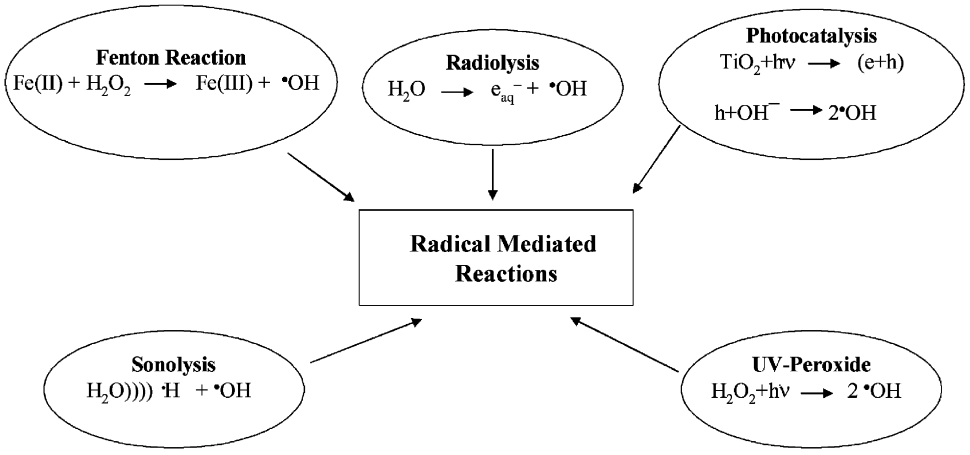

Fig. 1. Advanced oxidation processes.

Table 1
Advanced oxidation processes

No	Method	Reactive intermediates
1	Ozone treatment: O_3 or O_3/H_2O_2	$^{\bullet}OH$, $HO_2^{\bullet}/O_2^{-\bullet}$, $O_3^{-\bullet}$
2	Fenton processes: H_2O_2/Fe^{2+} or $H_2O_2/O_3/Fe^{2+}$ (acid media)	$^{\bullet}OH$, $HO_2^{\bullet}/O_2^{-\bullet}$, $O_3^{-\bullet}$
3	Photo-Fenton processes using UV light in addition	$^{\bullet}OH$
4	Photo-induced oxidation by UV ($\lambda = 185$ nm and 254 nm) or UV/O_3, UV/H_2O_2 and UV/O_3/H_2O_2, respectively, using e.g. low pressure Hg lamp	$^{\bullet}OH$, $HO_2^{\bullet}/O_2^{-\bullet}$, $O_3^{-\bullet}$
5	Photocatalytic treatment: UV/Vis light using TiO_2, ZnO, etc. as catalyst	$^{\bullet}OH$
6	Radiation-induced oxidation of pollutants using accelerated electrons, γ-rays, X-rays; synergistic effect in the presence of O_3/O_2, eventually H_2O_2 as additive	$^{\bullet}OH$, $HO_2^{\bullet}/O_2^{-\bullet}$, $O_3^{-\bullet}$, e_{aq}^-, $H^{\bullet}$
7	Electrochemical oxidation	
8	Ultrasonic treatment (sonolysis of water)	$^{\bullet}OH$, $^{\bullet}H$
9	Thermal oxidation used for liquid industrial wastes	

the oxidation of organic compounds are UV-peroxide, ozonation, the photo-Fenton process, photocatalysis, and sonolysis (see for example, Legrini et al., 1993; Pera-Titus et al., 2004; Forgacs et al., 2004) (Fig. 1 and Table 1). These methods are based on generation, and use of highly reactive intermediates, e.g., hydroxyl radicals as the primary oxidant for the decomposition of organic pollutants. A desirable goal may be the conversion of a pollutant into an easily degradable, non-toxic product (e.g., fuel or polymer) or mineralization.

In order to allow optimization of conditions, provide desired versatility and commercial competitiveness, it is necessary to understand the basic mechanisms of AOP: it is particularly important establishing the mechanisms of the free radical reactions in the remediation processes. The overall efficiency of remediation can be improved by controlling the reactivity and generation of free radicals. Pulse radiolysis (PR) is a unique tool for the generation of $^{\bullet}OH$ radicals and other powerful oxidants in aqueous solution and to study their reactions. Elegant mechanistic model studies were made based on this technique and the results can lead to a better understanding of AOP in complex environmental systems.

1.2. Radiolysis of aqueous solutions

In dilute dye solutions the hydrated electron (e_{aq}^-), hydroxyl radical ($^{\bullet}OH$) and hydrogen atom ($^{\bullet}H$) reactive intermediates of water radiolysis induce the decomposition of the solute:

$$H_2O \rightsquigarrow e_{aq}^-,\ {}^{\bullet}OH,\ {}^{\bullet}H\ G(e_{aq}^-) = 0.28;\quad G({}^{\bullet}OH) = 0.28;\ G({}^{\bullet}H) = 0.06. \tag{1}$$

G-values are the yields of primary intermediates in $\mu mol\,J^{-1}$ units.

By combining appropriately selected experimental conditions there are possibilities to reduce the kinds of primary reacting radicals, and therefore to obtain some information about the mechanism of undergoing reactions, or at least about the main possible reaction pathways (Spinks and Woods, 1990; Buxton et al., 1988; Woods and Pikaev, 1994):

- In N_2 or Ar saturated solutions between pH 3 and 11 the reaction takes place with $^{\bullet}OH$, $H^{\bullet}$ and e_{aq}^-.
- Below pH 2 in N_2 or Ar saturated solutions in nearly equal amounts $^{\bullet}OH$ radicals and $H^{\bullet}$ atoms are the primary reactive species. In the acidic pH range, e_{aq}^- is converted to $H^{\bullet}$ in reaction with hydroxonium ions: $e_{aq}^- + H_3O^+ \rightarrow H^{\bullet} + H_2O$.
- Reactions of $H^{\bullet}$ atoms are usually investigated in N_2 or Ar saturated solutions containing 0.2–1 $mol\,dm^{-3}$

tert-butanol below pH 2. The reaction between $H^\bullet$ and *tert*-butanol is slow: $H^\bullet + (CH_3)_3COH \rightarrow {}^\bullet CH_2(CH_3)_2COH + H_2$. In this system, the relatively unreactive radicals formed from *tert*-butanol are also present. The radicals form in the reaction: $^\bullet OH + (CH_3)_3COH \rightarrow {}^\bullet CH_2(CH_3)_2COH + H_2O$.

- Reactions of e^-_{aq} are studied in N_2 or Ar saturated solutions above pH 3 and in the presence of 0.2–1 mol dm^{-3} *tert*-butanol (there is a small contribution from the $H^\bullet$ atom reactions). Radicals formed from *tert*-butanol are also present.
- Reactions of $^\bullet OH$ radicals are investigated in N_2O saturated solution in the 3–11 pH range. In such solution, e^-_{aq} is converted to $^\bullet OH$ in the reaction $e^-_{aq} + N_2O + H_2O \rightarrow {}^\bullet OH + OH^- + N_2$. (At saturation the N_2O concentration is 0.025 mol dm^{-3} at room temperature.) There is a small (~10%) contribution from the $H^\bullet$ atom reactions.
- In air or oxygen saturated solutions the reactive species are the $^\bullet OH$ radicals, and the $O_2^{-\bullet}/HO_2^\bullet$ superoxide radical anion/perhydroxil radical pair that form in e^-_{aq} and $H^\bullet$ scavenging reaction by O_2 molecules ($e^-_{aq} + O_2 \rightarrow O_2^{-\bullet}$; $H^\bullet + O_2 \rightarrow HO_2^\bullet$). There is an acid/base equilibrium between the two species with a pK of 4.8: $O_2^{-\bullet} + H_3O^+ \leftrightarrow HO_2^\bullet + H_2O$.
- Solutions containing the *tert*-butanol and saturated with O_2 are used for studying the reactions of the $O_2^{-\bullet}/HO_2^\bullet$ pair.
- N_2O saturated solution above pH 3 containing *tert*-butanol give a possibility to study the reactions of $^\bullet CH_2(CH_3)_2COH$ radicals.

1.3. Properties of azo dyes

Among the dye classes which can be applied to cellulosic fibres, for which vat dyes, direct dyes and reactive dyes are the most important ones, the demand for reactive dyes is steadily growing. Their key properties are excellent wet fastness, brilliant shades, and simple application techniques.

Azo dyes are chemical compounds bearing the functional group R–N=N–R′ in which R and R′ are aryl groups. Because of the electron delocalization through the N=N group these compounds have vivid colours, such as red, orange, or yellow. The colour is dependent on the chromophore and the extent of conjugation. Depending on the number of azo groups there are mono-, di- and triazo dyes. Azo dyes generally are bound to the textile fibres through secondary bonds. The reactive dyes have active groups for chemically bonding to the textile. Such moieties are for instance the chlorine substituted triazine or the sulphatoethyl sulphonate groups. H-acid containing dyes belong to the class of reactive dyes.

H-acid has two acid–base transitions one of them is at low pH (pK_1 = 3.54) and this is due to the ionization of the amino group, and the other is connected with the ionization of the hydroxyl group (pK_2 = 8.64). We show these two possibilities in Scheme 1 (Pálfi et al., 2007).

The ionization of the $-SO_3H$ group is below pH 1. The substituents attached to H-acid slightly modify the pK-values (Bredereck and Schumacher, 1993).

As model compound in the following we often refer to Apollofix Red (AR-28, also called as CI. Reactive Red or CI. 18215, Scheme 2) a triazine and H-acid containing azo dye with intensive red colour, λ_{max} = 514, 532 nm, ε_{max} = 31400 mol^{-1} dm^3 cm^{-1} (Bredereck and Schumacher, 1993). The dye undergoes an acid dissociation at the OH group with pK = 11.74.

Azo dyes containing OH and azo group in neighbouring positions, like AR-28, exist in azo⇔hydrazone tautomer pair. We show an example for tautomerization, Scheme 3 and 4.

Below the pK value either of the two isomers may dominate, depending on the chemical structure of the dyestuff. In the case of *p*-substituted dyes the azo configuration very strongly prevails. When a phenyl group is attached to the –N=N– diazo group with a substituent in *o*-position (like for AR-28) the hydrazone tautomer dominates (Bredereck and Schumacher, 1993; Hihara et al., 2006).

In the case of H-acid containing dyes with secondary amino group (i.e. there is an H atom attached to the amino N atom), for instance AR-28, the H atom on N may also be involved in the tautomerizm (Scheme 4).

2. Experimental techniques

The degradation of high molecular mass dye compounds is rather complicated and for understanding the details of the processes highly sophisticated techniques are needed.

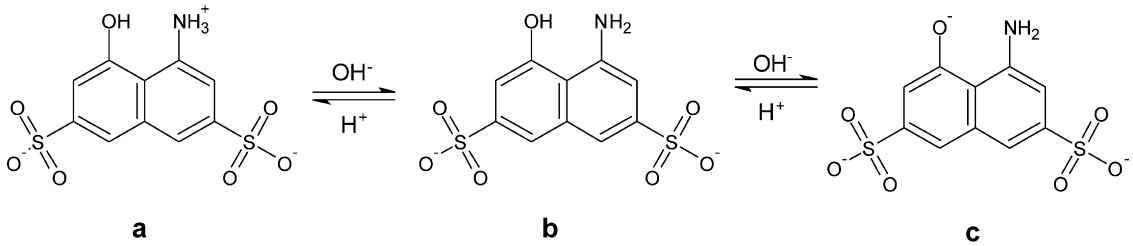

pK_1 = 3.54 pK_2 = 8.64

Scheme 1. Acid–base equilibria of H-acid.

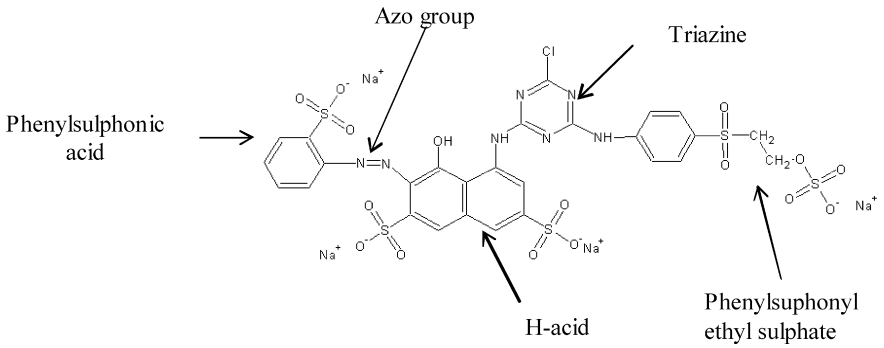

Scheme 2. Apollofix Red.

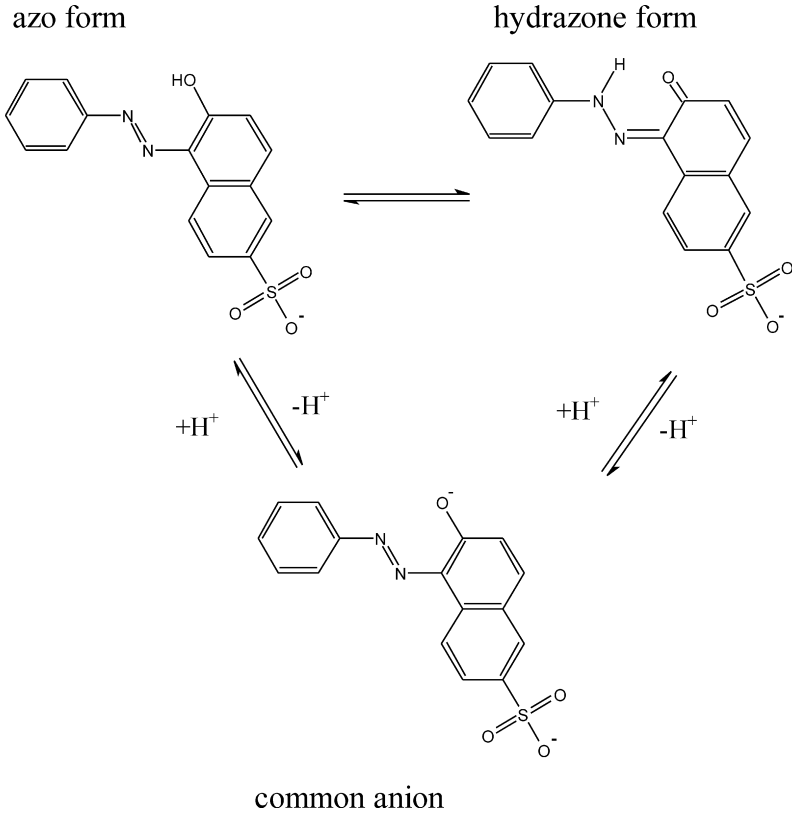

Scheme 3. Azo-hydrazone tautomerism exhibited by an arylazo-2-naphthol dye.

There was a great progress during the last decade in this field. The final degradation products are investigated by UV–Vis spectroscopy, HPLC chromatography, eventually combined with such detection methods as FTIR, MS, and NMR (Solpan and Güven, 2002; Butt et al., 2005; Huang et al., 2005; Wojnárovits et al., 2005a, b). The intermediates of transformations are studied by PR.

2.1. Steady-state techniques

2.1.1. Characterization of samples

For practical applications the treated samples can be characterized by such standardized methods as the determination of chemical oxygen demand (COD), biological oxygen demand (BOD), and total organic carbon content (TOC) (Majcen-Le Marechal et al., 1997; Han et al., 2002). Toxicity measurements are also of essential importance (Tezcanli-Guyer and Ince, 2003).

The values of COD, BOD and content of suspended solids (SS) are measured in accordance with standard methods (Eaton et al., 1995), utilizing dichromate method at closed reflux (for COD(Cr)), Wincler's azide modification method (for BOD), and weighting total filterable residue dried at 105 °C (for SS). Permanganate method in acid medium via standard procedure is utilized for measuring COD(Mn). TOC values are determined as a

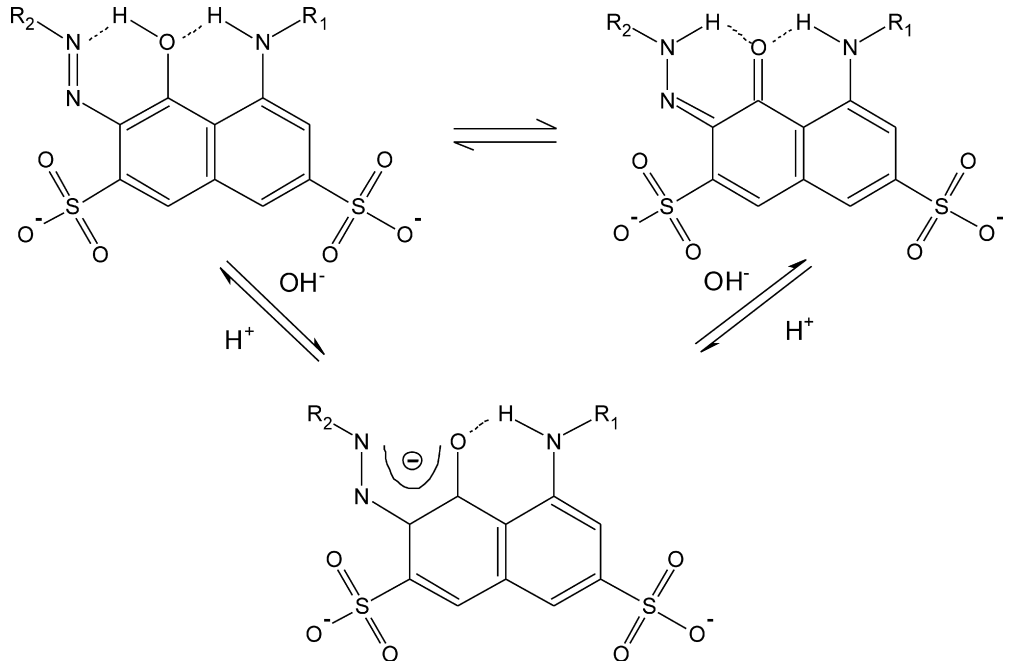

Scheme 4. Tautomerizm of AR-28.

difference between total carbon and inorganic carbon contents, both measured by registering CO_2 evolved due to catalytic incineration of dry residue and due to acidifying the solution by phosphoric acid, respectively.

Most of the papers published in the research field studied the decolouration curves using spectrophotometry. This is usually done by preparing appropriate solutions, treating them by stepwise irradiations and after each treatment taking the absorption spectra (Solpan et al., 2003). In radiolysis investigations this treatment is often done in a glass container, which has attached quartz cuvette for taking the absorption spectra in a spectrophotometer (Fig. 2). The cuvette should be made of good quality Suprasil quartz, which does not change its transparency during irradiation.

The degree of decolouration is usually calculated from the decrease of absorbance at a selected wavelength, most conveniently at the maximum absorbance by using

$$\text{Decolouration}\ (\%) = \frac{A_0 - A_i}{A_0} \times 100\%, \qquad (2)$$

where A_0 and A_i are the absorbances before and after the treatment, respectively.

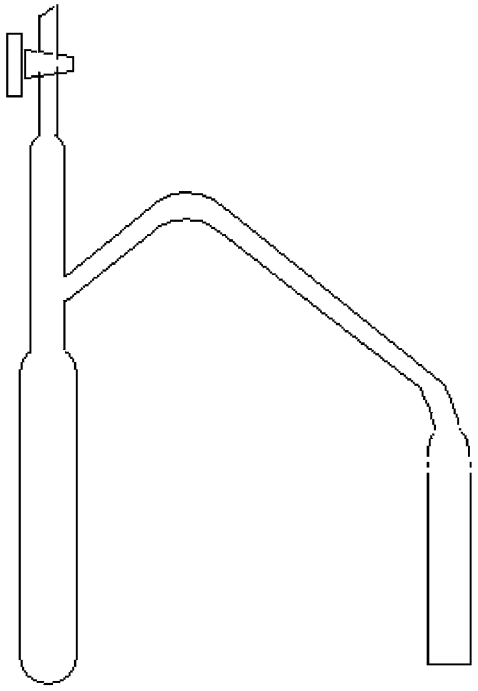

Fig. 2. Quartz cuvette used in decolouration experiments.

2.1.2. Separation and end-product detection

The chemical analysis of highly polaric molecules can be solved by applying HPLC with gradient ion-pair separation (Straub et al., 1992; Jandera et al. 1996; Holcapek et al., 2001; Kim et al., 2007). The identification of the separated products is rather complicated: identification based only on the absorption spectra is practically impossible. These absorption spectra are not characteristic enough, and several products may have very similar spectra. The separated components can be identified by FTIR, NMR, and MS techniques. For some of the dye molecules especially for the smaller molecular mass compounds GC–MS technique provide a good possibility for separation and identification.

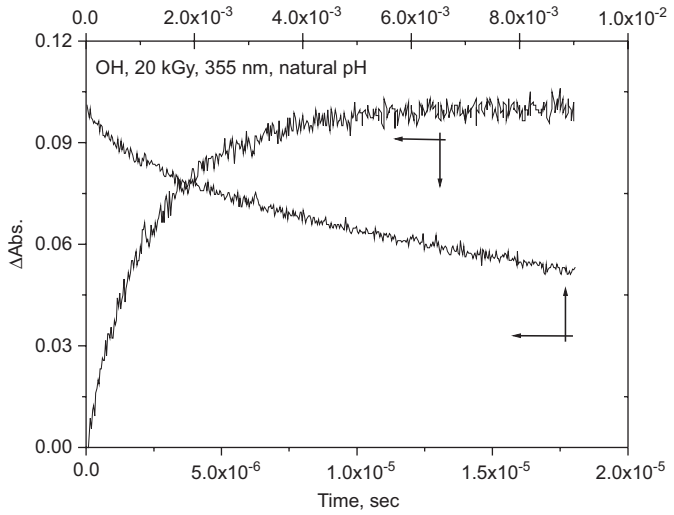

Fig. 3. Characteristic kinetic traces. Time dependence of the absorbance build-up and decay measured in pulse radiolysis experiments in 8.5×10^{-5} mol dm^{-3} AR-28 containing N_2O saturated solution with 20 kGy/pulse dose, at 355 nm, natural pH.

2.2. Pulse radiolysis technique

This method is applied to study the formation and decay of reactive transients under radiolytic conditions. A short pulse of accelerated electrons is used to initiate the primary chemical changes, the formation of reactive intermediates: radicals, ions and excited molecules. In the radiolysis of dilute aqueous dye solutions, hydrated electron (e_{aq}^-), hydroxyl radical ($^\bullet$OH) and hydrogen atom ($^\bullet$H) reactive primary intermediates induce the decomposition of the solute. The reaction of these primary intermediates with dye molecules results in formation of secondary (dye) intermediates. The concentration of these intermediates is followed by detecting their light absorption: the method is also called kinetic spectrophotometry. Kinetic curves (Fig. 3) are used to compute the spectra of intermediates. These spectra are characteristic to the intermediates formed and any change either in the shape of the spectrum or in the wavelength of the maximum indicates modification in the chemical structure.

From the kinetic curves, usually taken at the maximum of the spectrum on a short time-scale (ns or some μs), the rate coefficients of the addition of the radiolysis intermediates of the solvent to solute molecules are obtained (decay of primary intermediates and formation of secondary (dye) intermediates). Based on long time-scale measurements the rate coefficients of the disappearance of dye intermediates are calculated.

3. Radiolysis of model compounds

Our understanding of the mechanism of radiolysis of azo dyes is greatly enhanced by studies on model compounds. These model compounds, e.g., phenol, aniline, H-acid are usually the subparts of the practically applied dyes. The reactivity of the reducing species, e_{aq}^- and $^\bullet$H, in air-free media and also that of the oxidizing species, $^\bullet$OH, can be strongly affected by the molecular structure (e.g. by the substituents). This will be illustrated by individual compounds as examples.

3.1. Aniline and derivatives

Aniline (A, Scheme 5) reacts with $^\bullet$OH radicals with a rate coefficient of $\sim 1 \times 10^{10}$ mol^{-1} dm^3 s^{-1}. The reaction through an H-atom abstraction yields directly anilino radical ($C_6H_5NH^\bullet$, 36%), in addition *ortho*-directed OH-adduct forms (54%). The latter through water elimination gives also anilino radical: ($C_6H_5^\bullet(OH)NH_2 \rightarrow C_6H_5NH^\bullet + H_2O$). Some addition takes place on the *metha* and *ipso* positions. In PR experiments the decay of the transient absorption belonging to the $^\bullet$OH radical adduct of A also reveals that the absorption is caused by at least two transients (Christensen, 1972; Solar et al., 1986).

The H$^\bullet$ atom reacts with aniline in radical addition to the ring with a rate coefficient of 2×10^9 dm^3 mol^{-1} s^{-1} (Christensen, 1972; Solar et al., 1986). The reaction with hydrated electrons is very slow; the rate coefficient is 2.6×10^7 dm^3 mol^{-1} s^{-1}.

The $^\bullet$OH radicals react with *N,N'*-dimethylaniline (DMA) also with high rate coefficient, however, the mechanism of the reaction is different in DMA solution and in A solution. The fast first-order decay found in the A system was not found in the DMA system (Christensen, 1972). This may be due to a very fast decay of the $^\bullet$OH adduct not detectable by the applied instrument.

3.2. Phenol and derivatives

The investigation of radiation induced decomposition of benzene, phenol and their derivatives due to their environmental hazard is a rather popular subject and many papers have been published in this field (Land and Hanrahan, 2004; Gridkowski et al., 2004; Wasiewich et al., 2006; Kimura et al., 2006; Quint, 2006; Miyazaki et al., 2006a, b;

Aniline — **A**

N,N-Dimethylaniline — **DMA**

Scheme 5. Aniline and *N,N*-dimethylaniline.

Follut et al., 2007; Hu and Wang, 2007; Okamoto et al., 2007; Yang et al., 2007; Zhao et al., 2007). $^{\bullet}OH$ reacts with aromatic molecules with practically diffusion limited rate coefficient ($(1.0–1.4)\times10^{10}\,dm^3\,mol^{-1}\,s^{-1}$).

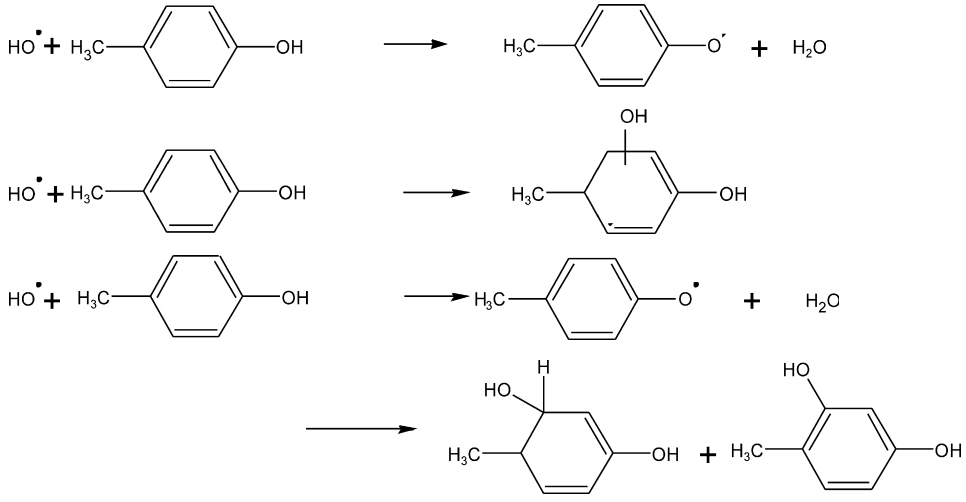

(3)

(4)

(5)

(6a)

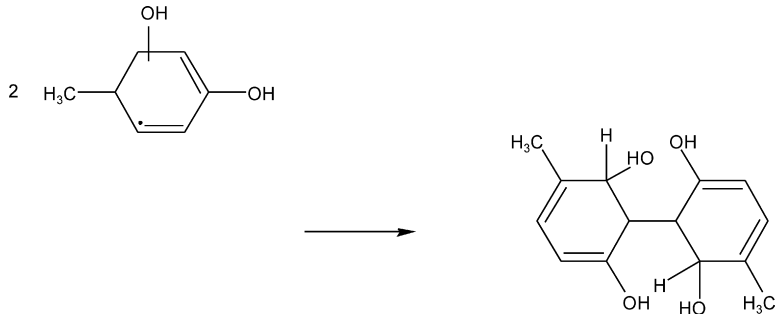

(6b)

The reaction with the OH group of phenols (we show this reaction in (3) below, on the example of *p*-cresol) and also with the alkyl substituents attached to the ring has relatively low rate coefficient.

The main reaction is the $^{\bullet}OH$ addition to any of the double bonds in the ring (4). Because $^{\bullet}OH$ is electrophilic reagent, it attacks mainly the electron-rich parts of the molecules. The cyclohexadienyl-type radical thus formed, in case of most of compounds, in neutral pH range is relatively stable and may decay in bimolecular radical–radical reactions (6). Reaction (6a) is disproportionation giving a cyclohexadiene-type compound and also a molecule with reformed aromatic structure. In (6b), a dimer with two cyclohexadiene-type parts is formed. Reaction (6) is in competition with unimolecular water elimination (5) resulting in a phenoxyl-type radical (Wojnárovits et al., 2002). The elimination reaction is an acid–base catalyzed reaction, therefore it is fast in acidic and basic solutions. The phenoxyl-type radicals are so called resonance-stabilized radicals with several mezomer forms.

In oxygen-containing solution, these reactions are in competition with the oxygen scavenging reaction (7) (Getoff, 1998, 2002):

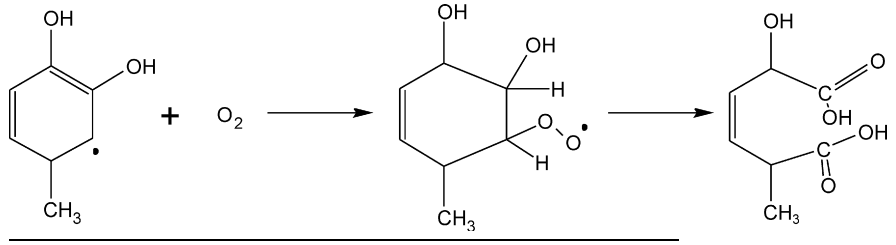

(7)

3.3. Azobenzene and derivatives

The transients formed in the attack of the solvated electron (e_{sol}^-) on *trans*-azobenzene (A), *trans*-4-nitroazobenzene (NA) and *trans*-4-diethylamino-azobenzene (DA, Scheme 6), have absorption maxima in the 375–650 nm range in methanol and in 2-propanol

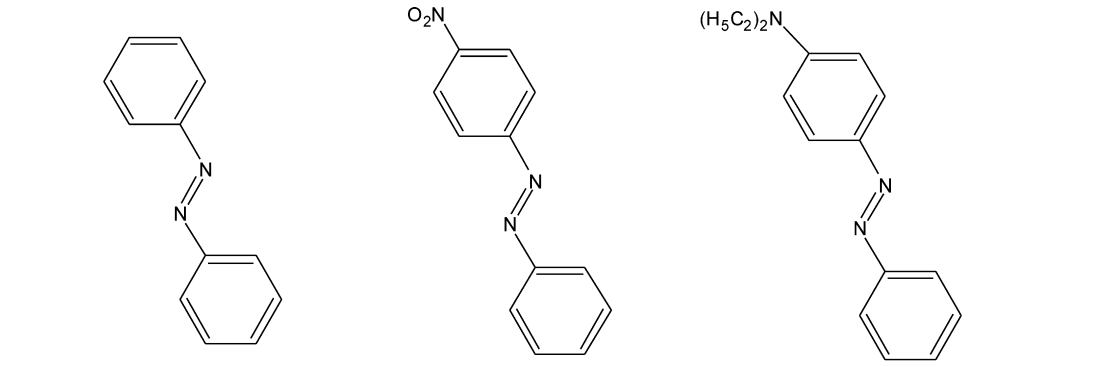

trans-azobenzene *trans*-4-nitroazobenzene *trans*-4-diethylamino-azobenzene

A **NA** **DA**

Scheme 6. Azobenzenes.

(Flamigni and Monti, 1985; Monti and Flamigni, 1986).

The rate coefficients are very high, they are in the range of $(1–2)\times10^{10}\,dm^3\,mol^{-1}\,s^{-1}$. Hydrazyl radicals are the primary species resulting from the rapid protonation of the corresponding anions (reaction (8)). $^{\bullet}CH_2OH$ radical does not react with A, but it reacts with DA to produce an adduct. $(CH_3)_2^{\bullet}CHOH$ can reduce A and DA at the azo-bond. The hydrazyl radicals of both substrates $AH^{\bullet}$ and $DAH^{\bullet}$ react with the parent compound to give dimer radicals $A_2H^{\bullet}$ and $DA_2H^{\bullet}$, respectively, in competition with other second-order processes. Subsequently, the dimer radicals undergo disproportionation with a low rate coefficient (10^6–$10^7\,dm^3\,mol^{-1}\,s^{-1}$):

$$-N=N- + e^-_{sol} \rightarrow -N=\!=-N- \xrightarrow{+H_2O} -N^{\bullet}-NH- + OH^-. \quad (8)$$

Azobenzene reacts with high rate coefficient with $^{\bullet}OH$ radicals (Panajkar and Mohan, 1993). About 40% of $^{\bullet}OH$ add to the benzene ring producing a transient with absorption maximum at 330 nm, and ~60% add to –N=N– double bond forming transient with maximum absorbance at 420 nm.

3.4. H-acid

The radiolysis of aqueous solutions of H-acid (Scheme 1) and one of its derivatives, which does not contain the $–NH_2$ group, was studied recently by pulsed radiolysis and end-product techniques (Pálfi et al., 2007). The radiation chemistry of the two compounds was found to be very similar with exception of $^{\bullet}OH$ reactions. $^{\bullet}OH$ radicals in reaction with H-acid partly abstract an H-atom from the $–NH_2$ group forming anilino-type radical. Both in the $^{\bullet}OH$ and e^-_{aq} addition reactions cyclohexadienyl-type radicals are produced. In the case of e^-_{aq} reactions first there is an addition to the ring, most probably to the one that contains the phenolic –OH group, and the cyclohexadienyl-type radicals form in a subsequent protonation. The $^{\bullet}OH$ radical addition presumably takes place to the other ring, especially in the case of H-acid, which contains the electron releasing $–NH_2$ group.

The intermediates decay on the ms timescale. In the case of H-acid the e^-_{aq}-adduct intermediate decayed faster while in the case of its derivative the decay of $^{\bullet}OH$ intermediate was more rapid. At a concentration of $0.25\,mmol\,dm^{-3}$ 6–8 kGy dose is sufficient to destruct the starting compounds. In the case of $^{\bullet}OH$ reactions, as a first step of decomposition hydroxylated molecules and quinone-type compounds form that absorb the light in the UV–Vis region. These molecules at higher doses by further decomposition of the ring structure transform to open chain alcohols, carboxylic acids, etc. In the case of e^-_{aq} even the primarily formed products have spectra shifted to the low-wavelength region indicating the destruction at least one of the C_6 rings. Relatively small doses are sufficient to degrade the starting non-biodegradable molecules to simpler biodegradable ones.

3.5. Triazines

s-Triazine derivatives, like atrazine have been and are still employed as herbicides. These compounds are of a ring structure characterized by strong aromacity and high chemical stability. Due to this high chemical stability under natural conditions their decomposition is very slow; therefore they cause a very long hazard for the environment.

The high-energy radiation induced decomposition of atrazine (Scheme 7) was studied by Karpel Vel Leitner et al. (1999) and Angelini et al. (2000). In end-product measurements atrazine showed extreme radiation stability. The attack of the intermediates of water radiolysis takes place on the substituents attached to the ring and there is hardly any change in the ring structure itself. The ring decomposition was observed at high doses. In transient measurements the triazine-type molecules were shown to

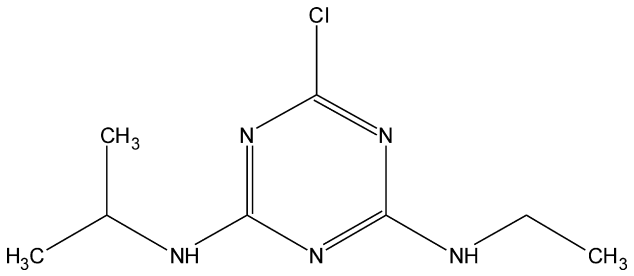

Scheme 7. Atrazine.

react with a relatively low-rate coefficient with the reactive intermediates of water radiolysis (DeLaat et al., 1994).

4. Degradation of azo dyes

Decolouration curves offer a convenient means to follow the radiolysis of dyes giving information on the disappearance of the starting molecules. However, the measurements cannot be applied to identify the products formed: for this purpose separation techniques are used. These techniques are needed also when the absorption spectra of the products strongly overlap with those of the starting compounds. The complete mineralization may be followed by TOC, BOD and COD measurements. In order to establish the mechanisms these techniques were complemented by the PR method for the observation of intermediates. Detailed studies are available on AR-28 and AO7 and in the following we often refer to these results.

4.1. Kinetic curves describing decolouration

In several papers the authors described the time dependence (or in radiolysis experiments the dose dependence) of the radiation or UV/H_2O_2-induced decolouration by using rate equations (Shu and Chang, 2006; Wang et al., 2006; Tezcanli-Guyer and Ince, 2003). As this point is critical and the applied kinetic methods are often ambiguous here we will detail this problem and put the treatment on firm kinetic basis (Wojnárovits and Takács, 2007; Wojnárovits et al., 2007).

Under steady-state conditions the following differential equation holds for the formation and decay of reactive intermediates:

$$\frac{d[I]}{dt} = r - [I]\left(\sum_{i=1}^{n} k_i[A_i]\right). \tag{9}$$

In the case of radiolysis the formation rate r is $GD_T\rho$, where G is the amount of reactive intermediates in mol, formed upon absorption of 1 J radiation energy (mol J^{-1}), D_T is the energy absorbed in 1 kg solution during 1 s time (J kg^{-1} s^{-1}), ρ is the density in kg dm^{-3}, the $[A_i]$'s are the concentrations of the dye molecules ($i = 1$) and their transformation products, $[I]$ is the concentration of reactive intermediate in mol dm^{-3}, the k_i's are the rate coefficients of the reactions between I and A_i.

At the beginning of the treatment (at lower doses) the dye concentration is higher by several orders of magnitude than the concentration of the reactive primary intermediates, therefore the formation rate of reactive primary intermediates is the rate-determining step and the equation can be simplified as:

$$\frac{d[I]}{dt} = r - [I]k_1[A_1]. \tag{10}$$

Under steady-state conditions the intermediate radicals form with a constant rate and they decay with the same rate:

$$r = [I]k_1[A_1]. \tag{11}$$

If we combine Eq. (11) with the differential equation used for describing the dye disappearance (Eq. (12)), we obtain a simple linear Eq. (13) for the dye destruction:

$$\frac{d[A_1]}{dt} = -[I]k_1[A_1], \tag{12}$$

$$[A_1] = [A_1]_{t=0} - rt = [A_1]_{t=0}\left(1 - \frac{r}{[A_1]_{t=0}}t\right) = [A_1]_{t=0}(1 - k_{obs}t). \tag{13}$$

In the equations $[A_1]_{t=0}$ and $[A_1]$ are the concentration of intact dye molecules at the beginning and at time t.

According to the latter equation, at the beginning of the decolouration the concentration of the intact dye molecules is linearly dependent on time. The slope (the pseudo-first-order rate coefficient) is the ratio of the rate of intermediate formation and the initial dye concentration. This initial linear dependence is a general phenomenon and it is also observed in the radiolysis of AR-28 as shown in Fig. 4b and d.

With progression of treatment the amount of the products increases continuously. The differential equations describing the process can be solved with some simplifications. However, there is a considerable difference whether the products also react with the primary intermediate with considerably high-rate coefficient or the reactivity of the products is low. For the case when the reactivity of the starting compound with the intermediate is high and that of the product is low, the equation can be written as

$$\frac{d[I]}{dt} = r - [I]\left(k_1[A_1] + \sum_{i=2} k_i[A_i]\right), \quad k_1[A_1] \gg \sum_{i=2} k_i[A_i], \tag{14}$$

$$\frac{d[I]}{dt} = r - [I]k_1[A_1] \simeq 0. \tag{15}$$

Combining Eq. (15) with Eq. (12), we obtain the same differential equation as before with solution of Eq. (13). Typically such higher linear region is observed when the intermediate reacts with high rate coefficient with the N=N double bond causing decolouration. Fig. 4d shows examples for this long linear region. With the progression

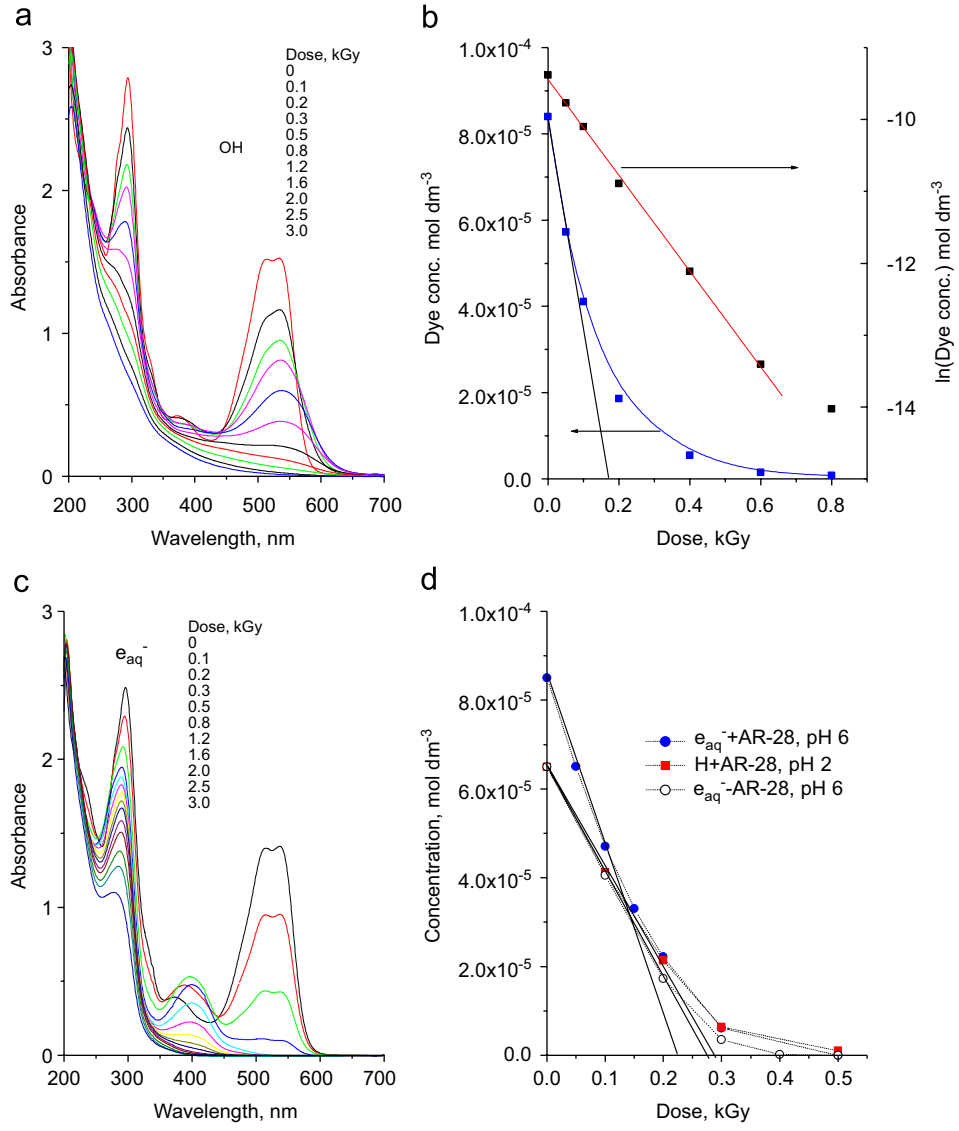

Fig. 4. Decolouration of 8.5×10^{-5} mol dm^{-3} concentration aqueous AR-28 solutions in the reactions of hydroxyl radicals in N_2O saturated solutions (a), the decrease of the dye concentration, measured by HPLC, as a function of dose (b). Dose dependence of decolouration (in N_2 saturated *tert*-butanol containing solution) caused by hydrated electron (c, d) and hydrogen atom reactions (d). (The measurements with 8.5×10^{-5} mol dm^{-3} initial concentration were carried out with HPLC separation and diode array detection and those with 6.5×10^{-5} mol dm^{-3} initial concentration with spectrophotometric evaluation (d).)

of the reaction the depletion of the dye gets so high that the reaction of the products (I+product) can compete with the I+dye reaction. At higher conversion the dependence deviates from linearity.

The kinetics completely changes when the intermediate reacts with high rate coefficients with both the starting molecules and also with the products. When the rate coefficient with both the dye and the products is practically diffusion limited for both reactions the same k rate coefficient can be used ($k \approx k_1 \approx \cdots \approx k_i$). For that reason, the rate equations may be written in the following form:

$$\frac{d[I]}{dt} = r - k[I]\left([A_1] + \sum_{i=2}^{n}[A_i]\right) \simeq 0. \tag{16}$$

We may write for the concentration of the products as

$$\sum_{i=2}^{n}[A_i] = [A_1]_{t=0} - [A_1]. \tag{17}$$

Using the last two equations and also Eq. (12), we obtain the time dependence shown in Eq. (19):

$$\frac{d[I]}{dt} = r - k[I][[A_1] + ([A_1]_{t=0} - [A_1])] \simeq 0, \tag{18}$$

$$[A_1] = [A_1]_{t=0}\exp\left(-\frac{r}{[A_1]_{t=0}}t\right) = [A_1]_{t=0}\exp(-k_{obs}t). \tag{19}$$

As Fig. 4b shows ln concentration is linearly dependent on dose in $^{\bullet}$OH-induced decomposition of AR-28.

As a summary, we can say that at very low conversion the concentration of the intact dye molecules is linearly dependent on the time of the treatment. At higher conversions in some cases the linearity remains, whereas in other cases the time dependence is logarithmic. If the reactivity of the primary intermediates with the intact molecules is high and with the products is low, there is a long linear dependence. When the reactivity is high with both the dye and the products the time dependence is logarithmic.

4.2. Transient intermediates (pulse radiolysis and theoretical calculations)

The kinetic curves measured by PR provide simple way to calculate the rate coefficients of water radical reactions with solute molecules. A large number of rate coefficients with some of model compounds and with dyes are collected in Table 2. From the relevant data it appears that the rate coefficients of OH radical reactions with the dyes and also with model compounds show very little variation with the molecular structure because all of the rate coefficients are close to the diffusion controlled limit ($1–1.4\times10^{10}\,mol^{-1}\,dm^3\,s^{-1}$). In case of the e^-_{aq} and $^{\bullet}H$ atom reactions there is a definite structure dependence. With other oxidizing radicals (not shown in the table), e.g. $N_3^{\bullet}$, the rate coefficients are much smaller and the values are dependent both on the structure of the dye and on the tautomeric form (Sharma et al., 2003). The efficiency of the one-electron oxidation of the different tautomeric forms of dyes was found to be in the order of common ion > hydrazone > azo. The efficiency of the reduction may follow a reverse order.

A general problem of the PR experiments in connection with dye destruction is the very strong overlap of the absorption spectra of the intermediates and that of the starting compounds, which complicates the measurements. As a result of pulsed energy absorption in the sample, some of the dye molecules transform to intermediates (mainly to radicals) so due to the reaction of dye molecules there is bleaching. On the other hand, the transients usually have strong light absorption in the visible range; in PR we measure the sum of the two effects: bleaching and product formation. The practically obtained spectra are the resultant of the two effects showing decrease of absorption in the visible region. The maximum of this decrease corresponds to the ground-state absorption maximum of the dye (Padmaja and Madison, 1999; Dajka et al., 2003). In order to obtain the transient absorption spectra of the intermediates correction techniques are applied (Sharma et al., 2002, 2003). The method developed by Wojnárovits et al. (2005a) is introduced below.

With a conventional spectrophotometer we measure the 'absolute' absorbance of the dye solution ($A_\lambda^{t=0}$) (see Fig. 5 and Fig. 6, curve a). In PR, we measure the time dependence of the absorbance difference between the absorbancies of the irradiated and not irradiated solutions ΔA_λ^t at selected wavelengths. The spectrum is composed of the ΔA_λ^t-values at a given time after the pulse (Fig. 6, lower part). The absolute absorbance at wavelength λ and at time t after the pulse is the sum of the absorbancies of the initial solution, $A_\lambda^{t=0}$, and ΔA_λ^t measured in PR:

$$A_\lambda^{t=0}+\Delta A_\lambda^t=A_\lambda^t+\sum_I^n \varepsilon_I c_I^t+\sum_p^m \varepsilon_p c_p^t. \tag{20}$$

The absorbance of the solution may be written as a linear combination of the absorbancies of the unreacted dye, $A_\lambda{}^t$, and those of the intermediates and final products. Eq. (21) is a rearranged form of Eq. (20). Eq. (21) shows that the sum of the absorbancies of the intermediates and final products is equal to the absorbance of the depleted dye, $A_\lambda^{t=0}-A_\lambda^t$, plus ΔA_λ^t:

$$\sum_I^n \varepsilon_I c_I^t+\sum_p^m \varepsilon_p c_p^t=A_\lambda^{t=0}-A_\lambda^t+\Delta A_\lambda^t, \tag{21}$$

where ε_I and ε_p are the extinction coefficients of the dye intermediates and final products and c_I and c_p are the respective concentrations. The Lambert–Beer low is used to calculate the absorbance with cell length of 1 cm. If we know the amount, or concentration of the dye depleted, by using Eq. (21) we can calculate the sum of absorbancies of the intermediates and final products.

A few μs after the pulse the reactive intermediates of water radiolysis have already reacted with the dye forming radical dye intermediates, but stable final products have not yet formed. So we can calculate the absorbance of the dye intermediates. On the other hand, taking the absorbance value at long times, a few hundred ms after the pulse, when the dye intermediates have already disappeared, we can calculate the absorbance of the final products.

In Fig. 6, we summarize the derivation of the spectrum of AR-28 intermediates: *a* shows the absorption spectrum of the initial solution taken with a conventional spectrophotometer having an intensive absorbance in the visible range. The lower part of Fig. 6 shows transient absorption spectra taken at time delays of 10 μs and 9 ms after the electron pulse in N_2O saturated solution where the $^{\bullet}OH$ radical reacts with the dye molecules (ΔA^t). In the transient spectrum there is an intensive bleaching after the pulse in the visible part of the spectrum between 460 and 585 nm due to the transformation of some part of the dye molecules absorbing in this range. After the initial bleaching, a part of the colour is regenerated during the time of the transient recording, 9 ms, due to the regeneration of the conjugated structure.

The sum of curve *b* (taken at 10 μs) and *a* is *c*, the "absolute" spectrum under PR conditions, and *d* is the derived spectrum of intermediates. The characteristic absorption bands between 300 and 400 nm can be attributed to cyclohexadienyl and naphthoxyl-type radicals.

The transient absorption spectrum formed in the reaction of e^-_{aq} with AR-28 is similar to that observed in the reaction of $^{\bullet}OH$ radical. It also shows the intensive decolouration between 450 and 585 nm, however, the

Table 2
Rate coefficients of $^{\bullet}OH$, e^-_{aq} and $^{\bullet}H$ reactions with some aromatic molecules and dyes (Notre Dame Radiation Chemistry Data Center, www.rcdc.nd.edu)

Compounds	k ($dm^3\,mol^{-1}\,s^{-1}$)		
	$^{\bullet}OH$	e^-_{aq}	$^{\bullet}H$
Model compounds			
Benzene	7.9×10^9	9.0×10^6	1.1×10^9
Toluene	5.1×10^9		
Phenol	6.6×10^9	3.0×10^7	1.7×10^9
2-Methylphenol	1.1×10^{10}		
4-Methylphenol	1.2×10^{10}	4.2×10^7	
2-Chlorophenol		1.2×10^{10}	
4-Nitrophenol	3.8×10^9		
N-Phenylhydroxylamine	1.5×10^{10}		
Aniline, pH basic	8.6×10^9	3.0×10^7	2×10^9
N,*N*′-Dimethylaniline	1.4×10^{10}		
Benzenesulphonamide		2.8×10^9	
3,4-Dimethylbenzenesulphonate ion		6.9×10^9	
Aniline-2,5-disulphonate ion		5.9×10^9	
Benzoic acid		2.1×10^9	
Azobenzene	2.0×10^{10}	3.3×10^{10}	
4-Nitroazobenzene		2.3×10^{10} Solvent MeOH	
Naphthalene	9.4×10^9	5.0×10^9	3.4×10^9
1-Aminonaphthalene-4-sulphonate ion	7.9×10^9	6.7×10^9	
1-Naphthol	1.3×10^{10}		
2-Naphthol	1.2×10^{10}		1×10^9
2-Naphthylamine		1.8×10^{10}	
Atrazine	2.4×10^9		

	k ($dm^3\,mol^{-1}\,s^{-1}$)	
Dyes	$^{\bullet}OH$	e^-_{aq}
Methyl Orange (Padmaja and Madison, 1999) 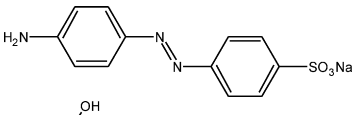	$(2\pm0.3)\times10^{10}$	
Calgamite (Padmaja and Madison, 1999) 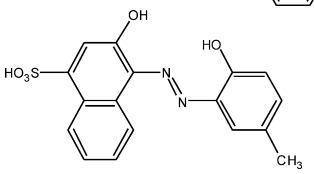	1.1×10^{10}	
Orange I (Sharma et al., 2003) 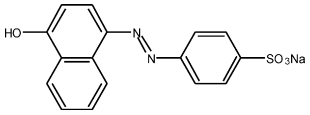	pH 4, 7×10^9 pH 6.6, 9×10^9 pH 10.5, 1.1×10^{10}	
Acid Orange 7 (Vinogdopal and Kamat, 1998) 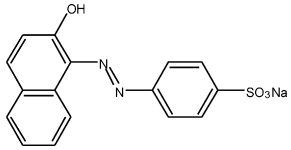	4.08×10^9	
Arylazo-2-naphthol (Sharma et al., 2002) 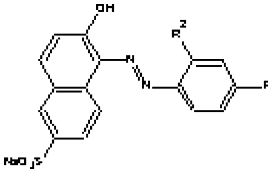		
$R^1=R^2=H$	1.1×10^{10}	2.5×10^{10}
$R^1=H$, $R^2=OCH_3$	1.0×10^{10}	1.5×10^{10}
$R^1=OCH_3$, $R^2=H$	1.1×10^{10}	8×10^9
$R^1=Cl$, $R^2=H$	1.0×10^{10}	1.9×10^{10}
$R^1=CH_3$, $R^2=H$	1.2×10^{10}	1.6×10^{10}

Table 2 (*continued*)

Compounds	k ($dm^3\,mol^{-1}\,s^{-1}$)		
	$^{\bullet}OH$	e^-_{aq}	$^{\bullet}H$
Naphthol Blue Black (Acid Black I, Nasr et al., 1997) 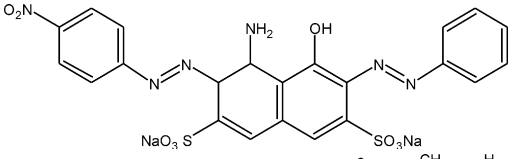			1.04×10^9
Acid Red 265 (Suzuki et al., 1975) 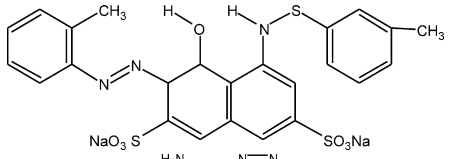	$(9.3 \pm 1.4) \times 10^9$		
Congo Red (C.I. Direct Red 28, Ma et al., 2007) 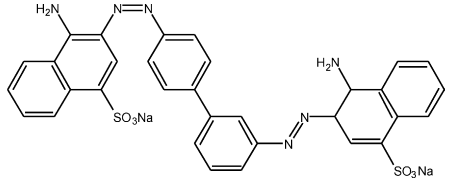	1.2×10^{10}	1.6×10^9 3.6×10^9	

absorbance above 600 nm is much weaker here than in the case of the $^{\bullet}OH$ adduct spectrum and also the regeneration of the absorbance in the visible range is smaller. This is in agreement with the conclusion based on the final product measurements that in the case of e_{aq}^- reactions there is an immediate destruction of the colour giving centre.

The spectra of the intermediates formed in the attack of the water radicals on the dye molecules allow the identification of the intermediates, i.e., allow the identification of the place of attack. In connection with the place of the primary attack also several theoretical calculations are published.

According to the frontier orbital theory, chemical reactions preferentially occur at the position of the molecule where their frontier orbitals strongly overlap. Nucleophilic reactions (e^-_{aq}, $H^{\bullet}$) may occur at the atom where the electron density of the lowest unoccupied molecular orbital (LUMO) is the largest, whereas electrophilic reactions ($^{\bullet}OH$) may occur at the position where the density of the highest occupied molecular orbital (HOMO) is the largest (Zhang et al., 2005a).

The products formed from arylazo-2-naphthol dyes (Scheme 3) and the mechanism of degradation is discussed in several papers. The analytical results are compared with the results of theoretical calculations. According to the electron densities of HOMO and LUMO calculated by Hihara et al. (2003), the neucleophilic reaction of AO7 (arylazo-2-naphthol-type dye) may occur primarily at the N atom bound to the naphthalene ring. The electrophilic attack by $^{\bullet}OH$ radical should occur at the N atom bound to the benzene ring and at the C atom where the naphthalene ring and the azo group link up. The electron densities of HOMO at the two positions are similar. The quantum mechanical molecular orbital calculations of Özen et al. (2003) using density functional theory are more or less in agreement with that of Hihara et al. (2003, 2006). They proposed that oxidative degradation of amino-substituted azo dyes occur through cleavage of N–N bond, following the $^{\bullet}OH$ radical addition to the chromophore. They suggested that the presence of hydrazone tautomers might be responsible for the involvement of C–N cleavage in the degradation of azo dyes.

4.3. Mechanism of degradation of azo dyes, degradation products

The results on azobenzenes were discussed in Section 3. There are detailed investigations in the literature also on higher molecular mass azo compounds. Here we mainly refer to the results on Apollofix Red (AR-28) and arylazo-2-naphthol-type dyes (AO7), the radiolysis of dilute solutions of these compounds was thoroughly investigated by pulse and gamma radiolysis, spectrophotometry and HPLC separation techniques.

In Fig. 4, the results of decolouration experiments with AR-28 are shown (Wojnárovits et al., 2005a, b). In Fig. 4a and b, the experiment was carried out in N_2O saturated system (oxidative conditions, the reactant is $^{\bullet}OH$) while in Fig. 4c and d the solution was deoxygenated by N_2 and *tert*-butanol was added to the system (reductive conditions, the reactant is e^-_{aq}, or $H^{\bullet}$).

Due to the irradiation the absorbance in the visible range decreases, the shape of the spectrum either remains unaltered or changes during the treatment. In the first case (see Fig. 4c), the dose dependence of absorbance shows a longer linear part kinetically described by Eq. (13)

(see Fig. 4d). Such behaviour may be due to the attack of primary intermediates to the chromophoric part of the molecule (e.g. –C–N═N–C– bridge connecting the two aromatic groups) resulting in an irreversible reaction here. This reaction leads to the destruction of the chromophore, i.e., the extensive conjugated electronic system. The products formed do not have considerable light absorption in the visible range (and may have low reactivity with reducing species). The linearity of the dose dependence persists until the main reaction of the given primary intermediate is the reaction that induces the chromophore decomposition. In such cases, as a result of the attack N_2 molecule elimination or splitting of the bond between the two N atoms may occur. The remaining aromatic molecules may show characteristic absorption below 400 nm. The other possibility is a partial or total saturation of the double bond between the two nitrogen atoms forming –C–NH–N═C– or –C–NH–NR–C– (where R an H atom or any other group).

In the radiolysis of AR-28, the dose dependence is linear when hydrated electrons or hydrogen atoms react with the monoazo dye. As Eq. (8) shows the hydrated electron attacks the azo group (in agreement with theoretical calculations mentioned before): in the reaction hydrazyl-type radical forms. The same radical forms in $H^\bullet$ atom addition reaction:

$$-N{=}N- + H^\bullet \rightarrow -N^\bullet-NH-. \quad (22)$$

Both hydrated electron and $H^\bullet$ atom addition leads to destruction of the conjugation through the –N═N– bond, and consequently to decolouration. In the partial saturation quinoidal structures are also expected: these molecules show relatively weak light absorption in 400–600 nm range. These quinoidal structures very easily decompose by thermal processes to simpler molecules. This phenomenon was supported by end-product measurements. HPLC analysis showed very sharp decrease in the concentration of the starting dye with the dose of irradiation. The products formed showed absorbance mostly in the UV region (Wojnárovits et al., 2005a, b).

The efficiency of decolouration in e^-_{aq} and $H^\bullet$ atom reactions was reported to be close to 100%. At longer reaction times (at higher doses), however, the dye is depleted so much that the e^-_{aq} and $H^\bullet$ intermediates of water radiolysis in higher proportion may not react with the azo moiety causing decolouration, but take part in other reactions, e.g., reacting with the products of radiolysis. For that reason, the time-dependence curve at higher depletion deviates from linearity (Fig. 4d).

When the reactant is $^\bullet$OH the spectra are changing during the treatment both in visible and UV regions, as shown in Fig. 4a by taking the example of AR-28 irradiated in N_2O saturated solution. The spectrum in the visible region gradually shifts to longer wavelengths. However, there is no clear isosbestic point, which shows that the starting compound does not transform quantitatively to coloured product. End-product analysis here also showed a sharp decrease in the concentration of the starting compound (Fig. 7a and b). However, the spectral characteristics and elution times of the new products are similar to that of the starting compound (Fig. 5), indicating that these are substituted versions of the starting compounds. This behaviour can be attributed to the complex structure of AR-28 offering several places to the $^\bullet$OH attack. Most possibly the radical attack takes places not only on the –N═N– double bond (as it was suggested by theoretical calculations) but also directly on the aromatic rings in different positions since the $^\bullet$OH radical reacts with practically diffusion limited rate coefficient ($k \approx 10^{10}$ $mol^{-1}\,dm^3\,s^{-1}$) with the aromatic rings and probably also with the –N═N– double bond (Figs. 6 and 7).

(The change in absorption spectra was also observed during the destruction of many other azo dyes (e.g. Suzuki et al., 1975, 1978; El-Assy et al., 1992; Tezcanli-Guyer and Ince, 2003; Zhang et al., 2005b; Wang et al., 2006; Földváry and Wojnárovits, 2007).)

The change of the absorption spectrum in the visible region is observed when the intermediates formed in the reaction of the water radicals and the dye molecules react with each other by re-establishing the conjugated system; however, the product molecules slightly differ from the starting molecules. In the case of the example shown in Fig. 4a, the $^\bullet$OH adduct cyclohexadienyl-type radicals by disproportionation yield product molecules that contain modified AR-28 molecules with an extra OH group (Wojnárovits et al., 2005a, b). Such reaction was shown on the example of *p*-cresol in reactions (6a) and (6b). If this extra OH-group is on the part of the dye molecule that is involved in the extensive conjugation, the spectrum in the visible range shifts to the red.

It is important to mention that all of the products that form in $^\bullet$OH radical reaction can again react with this radical. That is probably true for the product of the product, i.e., for the secondary product, tertiary product,

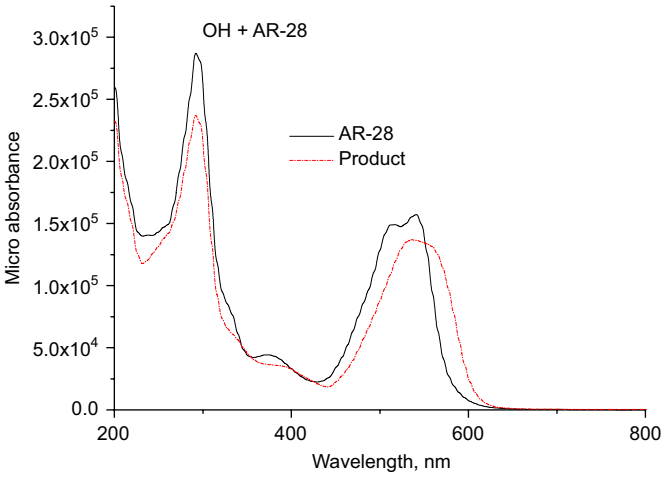

Fig. 5. Comparison of the absorption spectra of the dye and one of its main degradation product formed by $^\bullet$OH radical reaction. The spectra were recorded by using a diode-array detector after HPLC separation.

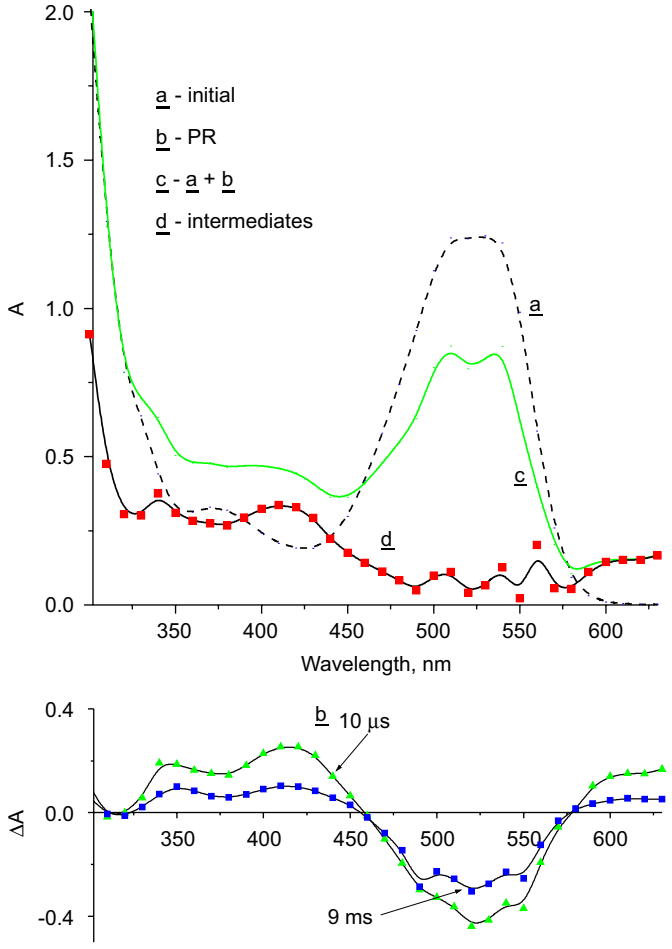

Fig. 6. Derivation of the absorption spectra of intermediates: (a) spectrum of the unirradiated solution taken with the UV–Vis spectrophotometer; (b) transient absorbance spectrum measured in pulse radiolysis; (c) the sum of *a* and *b* spectra, transient absorption spectrum; (d) the spectrum due to the unreacted AR-28 molecules subtracted from the transient spectrum *c*, this is the absorption spectrum of the intermediates.

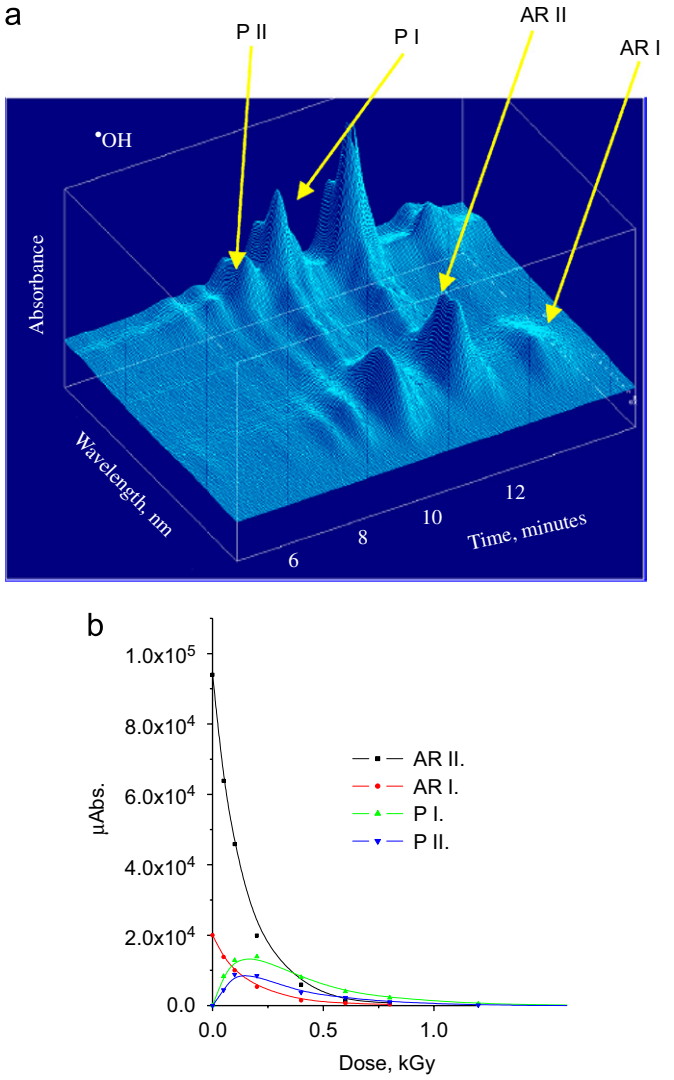

Fig. 7. Three-dimensional HPLC chromatogram showing the separation of components in N_2O saturated solution irradiated with 0.6 kGy dose (a). Destruction of AR-28 molecules and formation of degradation products in •OH radical reactions as detected by HPLC at 530 nm (b). AR I and AR II are used for AR-28 and for its hydrolysed form, respectively, PI and PII are products.

etc. With the progress of the reaction the number of colour giving intact and transformed molecules decreases and those of the transformed decoloured molecules increases. The competition between the •OH radical reaction with the decoloured and coloured products can explain the logarithmic-like decolouration curves described by Eq. (19) (Fig. 4b), often observed under circumstances when the •OH radical is the main reacting species.

Due to its complex structure the identification of products for such a large molecule as AR-28 is rather complicated and the analysis mostly identifies the type of compound formed. For some of the smaller dye molecules, which can be considered as the constituents of the larger ones, more detailed results are available.

As it was mentioned before under reductive and oxidative conditions the degradation mechanisms are different. These different mechanisms may lead to different products. The reductive attack of AO7 (arylazo-2-naphthol-type dye) leads to the formation of amino substituted compounds as it is shown in Scheme 8.

Under reductive conditions the first reaction steps are fast, however, the next degradation steps are rather slow (Zhang et al., 2005a).

Under oxidative conditions the reaction mechanism is more complicated, probably due to the further fast transformation of the primary degradation products. Different theories exist for the reaction mechanism. Vinogdopal and Kamat (1998) in their HPLC analysis on oxidative degraded samples of AO7 found one major, identifiable intermediate product, 4-hydroxybenzenesulphonic acid (HBS) with some traces of 1,2-naphthaquinone (Scheme 9). It is likely that naphthaquinone could undergo rapid oxidation to another product. The same result was obtained in photocatalytic, radiolytic and sonolytic decompositions.

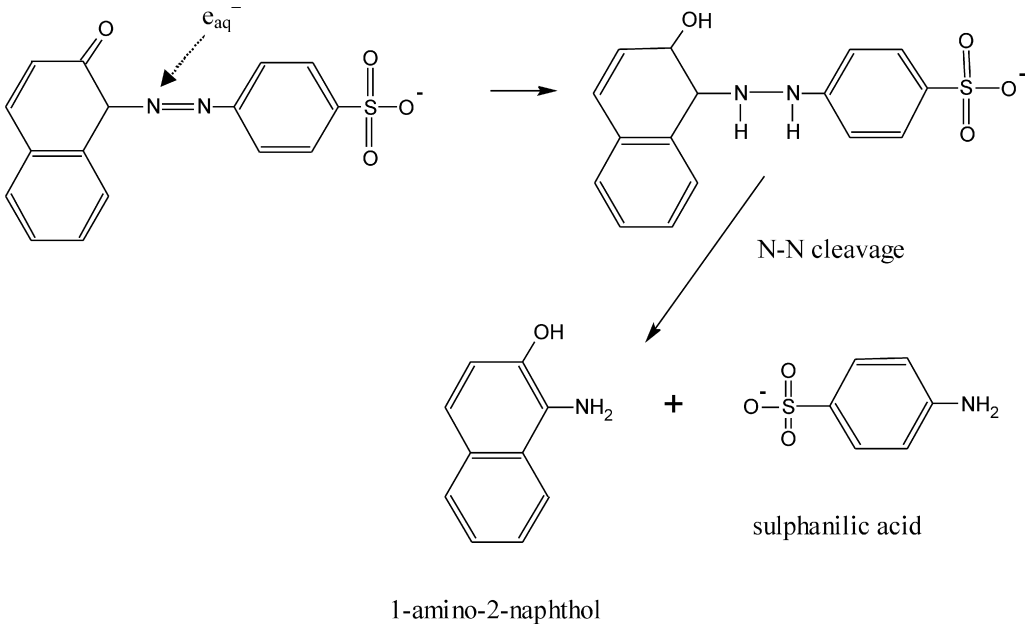

Scheme 8. Reductive degradation of AO7.

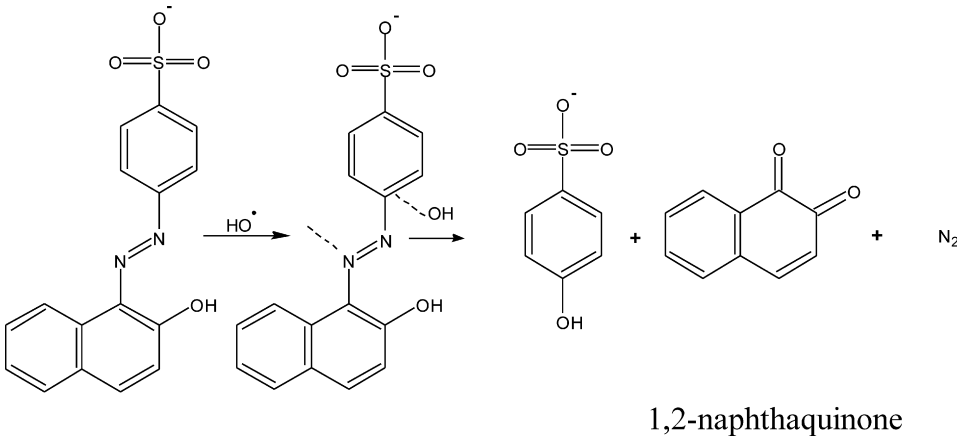

Scheme 9. Oxidative degradation of AO7.

In the light of their study on ^{14}C-labeled simple azo dyes, Spadaro et al. (1994) proposed that the $^{\bullet}OH$ radical produced by Fenton's reaction attacks the carbon atom bearing the azo leakage, leading to the cleavage of the C–N bond and the generation of benzene and phenyldiazene (Ph–N═NH) as intermediate. No Ph–N═NH formation is reported in experiments using sonochemical initiation (Joseph et al., 2000; Vinogdopal and Kamat, 1998). In the latter case, the extreme conditions (high pressure, gas–liquid interface) may facilitate immediate decomposition of labile products. By oxidizing azobenzenes and related azo dyes with combined sonochemical and Fenton reactions, Joseph et al. (2000) reported the oxidation of nitrogen to NO_x yielding nitroaromatic compounds. A portion of these products is able to partition within the gas phase inside the cavitation bubbles and undergo fast decomposition forming NO_2.

Concerning phenyldiazene product Coen and co-workers (2001) suggested a formation route through phenoxyl-type radical and then carbenium ion intermediate (Scheme 10).

In the case of *p*-phenylazoaniline, a simple compound that may mimic the real dyes, under oxidative conditions 4-aminophenol, aniline and phenol form (Scheme 11) as main products in addition to other not yet identified substances (Krapfenbauer et al., 2000). The product analysis suggests N_2 elimination and incorporation of OH at the place of the –N═N– group.

4.4. Mineralization

With the progression of the treatment under aerobic conditions the pH of the solution gradually decreases and tends to level off at constant value. The rate of lowering the pH is increasing with increasing oxygen

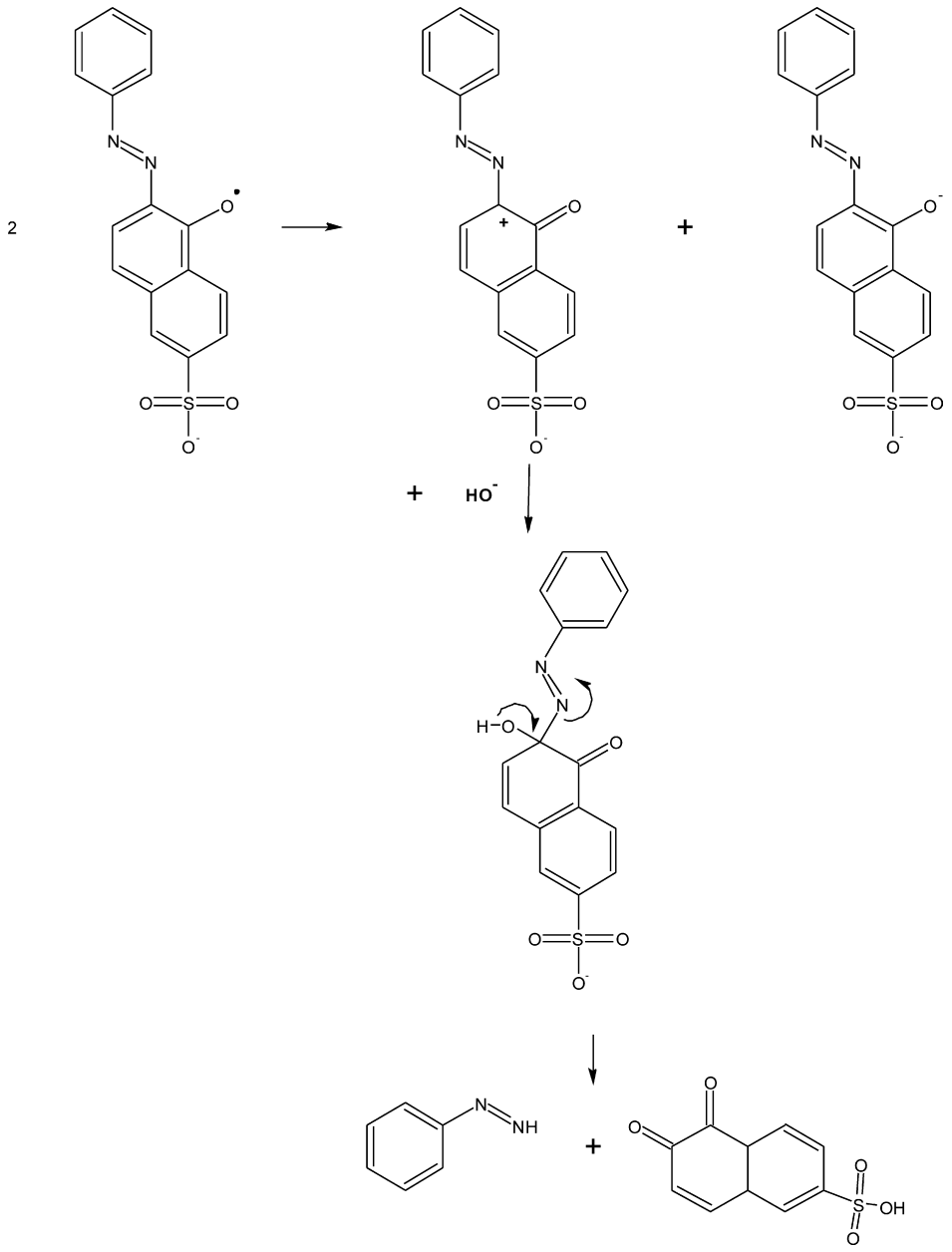

Scheme 10. Phenyldiazene formation in one-electron oxidation of phenylazo-2-naphthol.

concentration in the solution. This decrease of the pH is due to formation of organic acids, for instance dicarboxylic acids or acetic acid (reaction 7) (e.g. Vinogdopal et al., 1998; Zhang et al., 2005a; Hosono et al., 1993; Kim et al., 2007)).

Most of the dyes contain several aromatic rings and for that reason they have very strong absorbance around 230 nm, characteristic to aromatic compounds. While the decrease of absorbance in the visible region of the spectrum is due to the destruction of the extensive conjugation in the molecule (e.g. the destruction of conjugation through the –C–N═N–C– bridge), the decrease of absorbance at about 230 nm is directly related to the destruction of aromatic conjugation in the rings. As it was discussed before e^-_{aq} is very effective in decolourization (Sharma et al., 2003, Wojnárovits et al., 2005a, b)), and it is less active in the further degradation of the products formed. The effective reduction of absorbance in the UV region under aerobic conditions may be due to addition of $^{\bullet}OH$ radicals to aromatic rings followed by oxygen scavenging leading to cleavage of rings. In the absence of O_2 the absorbance reduction is small, this may be due to recovery of the aromatic rings attacked by addition of $^{\bullet}OH$ radicals through disproportionation reaction as it was shown before (see reactions (6a) and (6b)). The presence of oxygen in the solution induces a fixation of the damaged place and gives a possibility for ring opening yielding in the further reaction dicarboxylic acid.

From the available experimental evidences it seems that the ring opening reaction is determined by the oxygen diffusion.

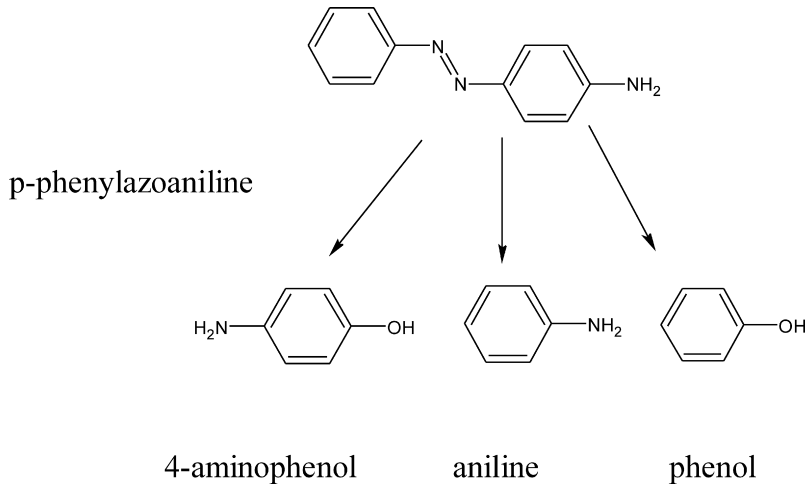

Scheme 11. Oxidative degradation products of *p*-phenylazoaniline.

The opened rings undergo further oxidation processes, and the final degradation products can be CO_2, H_2O and N_2 (or NH_4^+, NO_3^-, NO_2^- (Tanaka et al., 2000)). That process is called mineralization. The degree of mineralization is usually followed by the reduction of the TOC:

$$\text{Mineralization } \% = \frac{\text{TOC}_{\text{initial}} - \text{TOC}}{\text{TOC}_{\text{initial}}} 100\%. \quad (23)$$

The TOC reduction curves substantially differ from the decolouration curves (Kusic et al., 2006; Li et al., 2006). Although generally TOC reduction (i.e. mineralization) starts in the early stages of the treatment, during the decolouration period the TOC reduction is very small. It increases substantially after the colour disappeared.

4.5. Reactivity of the $O_2^{-\bullet}/HO_2^{\bullet}$ superoxide radical anion/perhydroxyl radical pair

When air is present during radiolysis the $O_2^{-\bullet}/HO_2^{\bullet}$ superoxide radical anion/perhydroxil radical pair always forms in e_{aq}^- and $H^\bullet$ scavenging reaction by O_2 molecules (see Section 1.2). This pair also forms in ozone decomposition in alkaline media, e.g., during wastewater treatment by combined irradiation and ozone technique.

$$O_3 + OH^- \rightarrow HO_2^\bullet + O_2^{-\bullet}, \quad (24a)$$

$$O_3 + OH^- \rightarrow {}^\bullet OH + O_3^{-\bullet}, \quad (24b)$$

$$O_3 + H_2O \rightarrow HO_3^+ + OH^- \Leftrightarrow 2HO_2^\bullet. \quad (25)$$

Since these species can easily be produced in radiolysis, PR is a convenient method to study their reactions. According to the general experiences, $HO_2^\bullet$ and $O_2^{-\bullet}$ are rather unreactive with the intact dye molecules (in general with aromatic molecules) (Krapfenbauer et al., 2000; Getoff, 2002; Wojnárovits et al., 2005a, b). However, they may react readily with some of the intermediate products in the mineralization process.

4.6. Practical applications of EB for dyeing wastewater treatment

Pilot plant and industrial scale experiments demonstrated the effectiveness of high-energy irradiation pre-treatment of wastewater when combined with conventional (mechanical screening, biological and chemical) methods. In most cases these plants were constructed to treat municipal wastewater (Pikaev, 1998), or industrial wastewater containing some organic pollutants (Sampa et al., 1995, 1998; Cooper et al., 1996; Buslaeva et al., 1991; Pikaev, 1998).

A pilot plant (output 1000 $m^3\,day^{-1}$) with ELV electron accelerator (energy 1 MeV, beam power 40 kW) for combined electron-beam and biological treatment of industrial textile dyeing wastewater is operating in Taegu Dyeing Industrial Complex (Daegu, Korea, Han et al., 1998, 2002) since 1998. This plant has shown considerable reduction of chemical additive consumption, and also a reduction in retention time, with an increase in removal efficiencies of COD and BOD. On the basis of data obtained from pilot plant operation, construction of an industrial scale plant was started in 2004, and finished in December 2005 (Han, 2006). The industrial plant is located on the area of an existing wastewater treatment facility and its capacity is 10,000 m^3 of wastewater per day. The facility is operating with 1 MeV, 400 kW accelerator and the radiation pre-treatment is combined with the existing biotreatment facility. The continuous operation of this facility will provide additional data on reliability and for a detailed economic evaluation.

Acknowledgements

We express our thanks to Hungarian Science Foundation (OTKA K 60 096). Support of the International Atomic Energy Agency (Contact no. 302-F2-HUN-12015) is also acknowledged.

References

Aksu, Z., 2005. Application of biosorption for the removal of organic pollutants: a review. Process Biochem. 40, 997–1026.

Angelini, G., Bucci, R., Carnevaletti, F., Colosimo, M., 2000. Radiolytic decomposition of aqueous atrazine. Radiat. Phys. Chem. 59, 303–307.

Bredereck, K., Schumacher, C., 1993. Structure reactivity correlations of azo reactive dyes based on H-acid. I. NMR chemical shift values, pK_a values, dyestuff aggregation and dyeing behaviour. Dyes Pigm. 21, 23–43.

Buslaeva, S.P., Vanyushkin, B.M., Gogolev, A.V., Kabakchi, S.A., Panin, Yu.A., Putilov, A.V., Upadyshev, L.B., 1991. Purification of aqueous solutions from non-biodegradable surfactants by accelerated electrons. Khim. Prom. 6, 47–50.

Butt, S.B., Qureshi, R.N., Shafaat, Q., 2005. Monitoring of radiolytic degradation of benzo(*a*)pyrene using γ-rays in aqueous media by HPLC. Radiat. Phys. Chem. 74, 92–95.

Buxton, G.V., Greenstock, C.L., Helman, W.P., Ross, A.B., 1988. Critical review of rate constants for reactions of hydrated electrons, hydrogen atoms and hydroxyl radicals ($^{\bullet}OH/O^{-\bullet}$) in aqueos solution. J. Phys. Chem. Ref. Data 17, 518–886. Updated version http://www.rcdc.nd.edu.

Christensen, H., 1972. Pulse radiolysis of aqueous solutions of aniline and substituted anilines. Int. J. Radiat. Phys. Chem. 4, 311–333.

Coen, J.J.F., Smith, A.T., Candeilas, L.P., Oakes, J., 2001. New insights into mechanisms of dye degradation by one-electron oxidation process. J. Chem. Soc., Perk. Trans. 2, 2125–2129.

Cooper, W.J., Dougal, R.A., Nickelsen, M.G., Waite, T.D., Kurucz, C.N., Lin, K., Bibler, J.P., 1996. Benzene destruction in aqueous waste. I. Bench-scale gamma irradiation experiments. Radiat. Phys. Chem. 48, 81–87.

Dajka, K., Takács, E., Solpan, D., Wojnárovits, L., Güven, O., 2003. High-energy irradiation treatment of aqueous solutions of C.I. Reactive Black 5 azo dye: pulse radiolysis experiments. Radiat. Phys. Chem. 67, 535–538.

DeLaat, J., Chramosta, N., Dore, M., Suty, H., Pouillot, M., 1994. Rate constants for reaction of hydroxyl radicals with some degradation by-products of atrazine by O_3 or O_3/H_2O_2. Environ. Technol. 15, 419–428.

Eaton, A.D., Clesceri, L.S., Greenberg, A.E. (Eds.), 1995. Standard Methods for the Examination of Water and Wastewater, 19th ed. American Public Health Association, American Water Works Association and Water Pollution Control Federation, Washington, DC.

El-Assy, N.B., Abdel-Rehim, F., Abdel-Gawad, A.S., Abdel-Fattah, A.A., 1992. The radiation-induced degradation of a diazo dye in aqueous solution, II. J. Radioanal. Nucl. Chem., Articles 157, 133–141.

Flamigni, L., Monti, S., 1985. Primary processes in the reduction of azo dyes in alcohols studied by pulse radiolysis method. J. Phys. Chem. 89, 3702–3707.

Follut, F., Pellizzari, F., Karpel Vel Leitner, N., Legube, B., 2007. Modelling of phenol removal in aqueous solution depending on the electron beam energy. Radiat. Phys. Chem. 76, 827–833.

Forgacs, E., Cserháti, T., Oros, G., 2004. Removal of synthetic dyes from wastewaters: a review. Environ. Int. 30, 953–971.

Földváry, Cs.M., Wojnárovits, L., 2007. The effect of high-energy radiation on aqueous solution of Acid Red 1 textile dye. Radiat. Phys. Chem. 76, 1485–1488.

Getoff, N., 1998. The role of peroxyl radicals and related species in the radiation-induced degradation of water pollutants. In: Cooper, W.J., Curry, R.D., O'Shea, K.E (Eds.), Environmental Applications of Ionizing Radiation. Wiley, New York, pp. 231–246.

Getoff, N., 2002. Factors influencing the efficiency of radiation-induced degradation of water pollutants. Radiat. Phys. Chem. 65, 437–446.

Gridkowski, J., Mirkowski, J., Plusa, M., Getoff, N., Popov, P., 2004. Pulse radiolysis of aqueous diphenyloxide. Radiat. Phys. Chem. 69, 368–379.

Han, B., 2006. Personal communication. (Bumsoo Han, EB-TECH CO., LTD. Republic of Korea, E-mail: bshan@eb-tech.com)

Han, B., Kim, D.K., Pikaev, A.K., 1998. Research activities of Samsung Heavy Industries in the conservation of the environment. In: Radiation Technology for the Conservation of the Environment, Proceedings of the Symposium held in Zakopane, Poland, 8–12 September 1997, IAEA, Vienna, pp. 339–347.

Han, B., Ko, J., Kim, J., Kim, Y., Chung, W., Makarov, I.E., Ponomarev, A.V., Pikaev, A.K., 2002. Combined electron-beam and biological treatment of dyeing complex wastewater. Pilot plant experiments. Radiat. Phys. Chem. 64, 53–59.

Hihara, T., Okada, Y., Morita, Z., 2003. Reactivity of phenylazonaphthol sulfonates, their estimation by semiempirical molecular orbital PM5 method, and the relation between their reactivity and azo-hydrazone tautomerism. Dyes Pigm. 59, 201–222.

Hihara, T., Okada, Y., Morita, Z., 2006. Photo-oxidation of pyrazolinylazo dyes and analysis of reactivity as azo and hydrazone tautomers using semiempirical molecular orbital PM5 method. Dyes Pigm. 69, 151–176.

Holcapek, M., Jandera, P., Zderadicka, P., 2001. High performance liquid chromatography–mass spectrometric analysis of sulphonated dyes and intermediates. J. Chromatogr. A 926, 175–186.

Hosono, M., Arai, H., Aizawa, M., Yamamoto, I., Shimizu, K., Sugiyama, M., 1993. Decoloration and degradation of azo dye in aqueous solution supersaturated with oxygen by irradiation of high-energy electron beams. Appl. Radiat. Isot. 44, 1199–1203.

Hu, J., Wang, J., 2007. Degradation of chlorophenols in aqueous solution by gamma irradiation. Radiat. Phys. Chem. 76, 1489–1492.

Huang, M., Russo, R., Fookes, B.G., Sigman, M.E., 2005. Analysis of fiber dyes by liquid chromatography mass spectrometry (LC–MS) with electrospray ionization: discriminating between dyes with indistinguishable UV–visible absorption spectra. J. Forensic Sci. 50, 526–534.

Jandera, P., Fischer, J., Stanek, V., Kucerova, M., Zvonicek, P., 1996. Separation of aromatic sulphonic acid dye intermediates by high-performance liquid chromatography and capillary zone electrophoresis. J. Chromatogr. A 738, 201–213.

Joseph, J.M., Destaillats, H., Hung, H.-M., Hoffmann, M.R., 2000. The sonochemical degradation of azobenzene and related azo dyes: rate enhancements via Fenton's reactions. J. Phys. Chem. A 104, 301–307.

Karpel Vel Leitner, N., Bergera, P., Gehringer, P., 1999. γ-irradiation for the removal of atrazine in aqueous solution containing humic substances. Radiat. Phys. Chem. 55, 317–322.

Kim, T-H., Lee, J.-K., Lee, M.-J., 2007. Biodegradability enhancement of textile wastewater by electron beam irradiation. Radiat. Phys. Chem. 76, 1037–1041.

Kimura, A., Taguchi, M., Ohtani, Y., Takigami, M., Shimada, Y., Kojima, T., Hiratsuka, H., Namba, H., 2006. Decomposition of *p*-nonylphenols in water and elimination of their estrogen activities by ^{60}Co γ-ray irradiation. Radiat. Phys. Chem. 75, 61–69.

Krapfenbauer, K., Wolfger, H., Getoff, N., Hamblett, I., Navaratnam, S., 2000. Pulse radiolysis and chemical analysis of azo dyes in aqueous solution I. *p*-phenylazoaniline. Radiat. Phys. Chem. 58, 21–27.

Kusic, H., Koprivanac, N., Srsan, L., 2006. Azo dyes degradation using Fenton type processes assisted by UV irradiation: a kinetic study. J. Photochem. Photobiol. A. Chem. 181, 195–202.

Land, L.L., Hanrahan, R.J., 2004. Exhaustive radiolysis of 11 mM aqueous benzene solutions: effect of added oxygen. Radiat. Phys. Chem. 69, 401–410.

Legrini, O., Oliveros, E., Braun, A.M., 1993. Photochemical process for water treatment. Chem. Rev. 93, 671–698.

Li, G., Qu, J., Zhang, X., Liu, H., Liu, H., 2006. Electrochemically assisted photocatalytic degradation of Orange II: influence of initial pH values. J. Mol. Catal. A: Chem. 259, 238–244.

Ma, H., Wang, M., Yang, R., Wang, W., Zhao, J., Shen, Z., Yao, S., 2007. Radiation degradation of Congo Red in aqueous solution. Chemosphere 68, 1098–1104.

Majcen-Le Marechal., A., Slokar, Y.M., Taufer, T., 1997. Decoloration of chlorotriazine reactive azo dyes with H_2O_2/UV. Dyes Pigm. 33, 281–298.

Miyazaki, T., Katsumura, Y., Lin, M., Muroya, Y., Kudo, H., Taguchi, M., Asano, M., Yoshida, M., 2006a. Radiolysis of phenol in aqueous solution at elevated temperatures. Radiat. Phys. Chem. 75, 408–415.

Miyazaki, T., Katsumura, Y., Lin, M., Muroya, Y., Kudo, H., Asano, M., Yoshida, M., 2006b. γ-radiolysis of benzophenone aqueous solution at elevated temperatures up to supercritical condition. Radiat. Phys. Chem. 75, 218–228.

Monti, S., Flamigni, L., 1986. Primary processes in the reduction of 4-nitroazobenzene. A pulse radiolysis study in alcoholic solvents. J. Phys. Chem. 90, 1179–1184.

Nasr, C., Vinogdopal, K., Hotchandani, S., Chattopadhyay, A.K., Kamat, P.V., 1997. Excited states and reduced and oxidized forms of a textile diazo dye, Naphthol Blue Black. Spectral characterization using laser flash photolysis and pulse radiolysis studies. Radiat. Phys. Chem. 49, 159–166.

Okamoto, K., Kozawa, T., Saeki, A., Yoshida, Y., Tagawa, S., 2007. Subpicosecond pulse radiolysis in liquid methyl-substituted benzene derivatives. Radiat. Phys. Chem. 76, 818–826.

Özen, A.S., Aviyente, V., Klein, R.A., 2003. Modeling the oxidative degradation of azo dyes: a density functional theory study. J. Phys. Chem. A 17, 4898–4907.

Padmaja, S., Madison, S.A., 1999. Hydroxyl radical-induced oxidation of azo dyes: a pulse radiolysis study. J. Phys. Org. Chem. 12, 221–226.

Pálfi, T., Takács, E., Wojnárovits, L., 2007. Degradation of H-acid and its derivative by ionizing radiation. Water Res. 41, 2533–2540.

Panajkar, M.S., Mohan, H., 1993. Investigations of transients produced on reactions of $^{\bullet}OH$ radicals with azobenzenes in aqueous solutions. Indian J. Chem. 32A, 25–27.

Pera-Titus, M., Garcia-Molina, V., Banos, M.A., Gimenez, J., Esplugas, S., 2004. Degradation of chlorophenols by means of advanced oxidation processes: a general review. Appl. Catal. B. Environ. 47, 219–256.

Pikaev, A.K., 1998. Electron-beam purification of water and wastewater. In: Cooper, W.J., Curry, R.D., O'Shea, K.E. (Eds.), Environmental Applications of Ionizing Radiation. Wiley, New York, pp. 495–506.

Quint, R.M., 2006. γ-Radiolysis of aqueous 2-chloroanisole. Radiat. Phys. Chem. 75, 34–41.

Sampa, M.H.O., Borrely, S.I., Vieira, J.M., Rela, P.R., Calvo, W.A.P., Duarte, C.L., Perez, H.E.B., Lugao, A.B., 1995. The use of electron beam accelerator for the treatment of drinking water and wastewater in Brazil. Radiat. Phys. Chem. 46, 1143–1146.

Sampa, M.H.O., Duarte, C.L., Rela, P.R., Somessari, E.S.R., Silveira, C.G., Azevedo., A.L., 1998. Remotion of organic compounds of actual industrial effluents by electron beam irradiation. Radiat. Phys. Chem. 52, 365–369.

Sharma, K.K., Rao, B.S.M., Mohan, H., Mittal, J.P., Oakes, J., O'Neill, P., 2002. Free-radical-induced oxidation and reduction of 1-arylazo-2-naphthol dyes: a radiation chemical study. J. Phys. Chem. A 106, 2915–2923.

Sharma, K.K., O'Neill, P., Oakes, J., Batchelor, S.N., Rao, B.S.M., 2003. One-electron oxidation and reduction of different tautomeric forms of azo dyes: a pulse radiolysis study. J. Phys. Chem. A 107, 7619–7628.

Shu, H.-Y., Chang, M.-C., 2006. Development of rate expression for predicting decolorization of C.I. Acid Black 1 in a UV/H_2O_2 process. Dyes Pigm. 70, 31–37.

Solar, S., Solar, W., Getoff, N., 1986. Resolved multisite OH-attack on aqueous aniline studied by pulse radiolysis. Radiat. Phys. Chem. 28, 229–234.

Solpan, D., Güven, O., 2002. Decoloration and degradation of some textile dyes by gamma irradiation. Radiat. Phys. Chem. 65, 549–558.

Solpan, D., Kölge, Z., 2006. Adsorption of methyl violet in aqueous solutions by poly(*N*-vinylpyrrolidone-co-methacrylic acid) hydrogels. Radiat. Phys. Chem. 75, 120–128.

Solpan, D., Güven, O., Takács, E., Wojnárovits, L., Dajka, K., 2003. High-energy irradiation treatment of aqueous solutions of azo dyes: steady-state gamma radiolysis experiments. Radiat. Phys. Chem. 67, 531–534.

Spadaro, J.T., Isabelle, L., Renganathan, V., 1994. Hydroxyl radical mediated oxidation of azo dyes: evidence for benzene generation. Environ. Sci. Technol. 28, 1389–1393.

Spinks, J.W.T., Woods, R.J., 1990. An Introduction to Radiation Chemistry, third ed. Wiley-Interscience, New York.

Straub, R., Voyksner, R.D., Keever, J.T., 1992. Thermospray, particle beam and electrospray liquid chromatography–mass spectrometry of azo dyes. J. Chromatogr. 627, 173–186.

Suzuki, N., Nagai, T., Hotta, H., Washino, M., 1975. The radiation-induced decoloration of azo dye in aqueous solution. Bull. Chem. Soc. Japan 48, 2158–2163.

Suzuki, N., Miyata, T., Sakumoto, A., Hashimoto, S., Kawakami, W., 1978. The degradation of an azo dye in aqueous solution by high-intensity electron beam irradiation. Int. J. Appl. Radiat. Isot. 29, 103–108.

Tanaka, K., Padermpole, K., Hisanaga, T., 2000. Photocatalytic degradation of commercial azo dyes. Water Res. 34, 327–333.

Tezcanli-Guyer, G., Ince, N.H., 2003. Degradation and toxicity reduction of textile dyestuff by ultrasound. Ultrason. Sonochem. 10, 235–240.

Vinogdopal, K., Kamat, V.P., 1998. Hydroxyl-radical-mediated oxidation: a common pathway in the photocatalytic, radiolytic, and sonolytic degradation of textile dyes. In: Cooper, W.J., Curry, R.D., O'Shea, K.E. (Eds.), Environmental Applications of Ionizing Radiation. Wiley, New York, pp. 588–599.

Vinogdopal, K., Peller, J., Makogon, O., Kamat, P., 1998. Ultrasonic mineralization of a reactive textile azo dye, Remazol Black B. Water Res. 32, 3646–3650.

Wang, M., Yang, R., Wang, W., Shen, Z., Bian, S., Zhu, Z., 2006. Radiation-induced decomposition and decoloration of reactive dyes in the presence of H_2O_2. Radiat. Phys. Chem. 75, 286–291.

Wasiewich, W., Chmielewski, A.G., Getoff, N., 2006. Radiation-induced degradation of aqueous 2,3-dihydroxynaphthalene. Radiat. Phys. Chem. 75, 201–209.

Wojnárovits, L., Takács, E., 2007. Development of rate expression for predicting decolorization of C.I. Acid Black 1 in a UV/H_2O_2 process. Dyes Pigm. 75, 505–506.

Wojnárovits, L., Földiák, G., D'Angelantonio, M., Emmi, S.S., 2002. Mechanism of OH radical-induced oxidation of *p*-cresol to *p*-methylphenoxyl radical. Res. Chem. Intermed. 28, 373–386.

Wojnárovits, L., Takács, E., Pálfi, T., 2005a. Radiolysis of azo dyes in aqueous solution: Apollofix Red. Res. Chem. Intermed. 31, 679–690.

Wojnárovits, L., Pálfi, T., Takács, E., Emmi, S.S., 2005b. Reactivity differences of hydroxyl radicals and hydrated electrons in destructing azo dyes. Radiat. Phys. Chem. 74, 239–246.

Wojnárovits, L., Pálfi, T., Takács, E., 2007. Kinetics and mechanism of azo dye destruction in Advanced Oxidation Processes. Radiat. Phys. Chem. 76, 1497–1501.

Woods, R.J., Pikaev, A.K., 1994. Applied Radiation Chemistry. Radiation Processing. Wiley, New York.

Yang, R., Wang, M., Shen, Z., Wang, W., Ma, H., Gu, J., 2007. The degradation and mineralization of 4-chlorophenol in aqueous solutions by electron beam irradiation in the presence of TiO_2 nanoparticles. Radiat. Phys. Chem. 76, 1122–1125.

Zhang, S-J., Yu, H-Q., Li., Q-R., 2005a. Radiolytic degradation of Acid Orange 7: a mechanistic study. Chemosphere 61, 1003–1011.

Zhang, S-J., Yu, H-Q., Zhao, Y., 2005b. Kinetic modeling of the radiolytic degradation of Acid Orange 7 in aqueous solutions. Water Res. 39, 839–846.

Zhao, C., Hirota, K., Taguchi, M., Takigami, M., Kojima, T., 2007. Radiolytic degradation of octachlorodibenzo-*p*-dioxin and octachlorodibenzofuran in organic solvents and treatment of dioxin-containing liquid wastes. Radiat. Phys. Chem. 76, 37–45.